

**MULTI-STAGE POPULATION MODELS APPLIED TO INSECT
DYNAMICS**

Antone dos Santos Benedito

Thesis presented to São Paulo State
University (UNESP) for the degree of
Doctor of Biometry.

BOTUCATU
São Paulo - Brazil
February 2020

**MULTI-STAGE POPULATION MODELS APPLIED TO INSECT
DYNAMICS**

Antone dos Santos Benedito

Adviser: **Cláudia Pio Ferreira**

Co-adviser: **Odair Aparecido Fernandes**

Thesis presented to São Paulo State
University (UNESP) for the degree of
Doctor of Biometry.

BOTUCATU
São Paulo - Brazil
February 2020

B463m Benedito, Antone dos Santos
Multi-stage population models applied to insect
dynamics / Antone dos Santos Benedito. -- Botucatu, 2020
60 p.

Tese (doutorado) - Universidade Estadual Paulista
(Unesp), Instituto de Biociências, Botucatu
Orientadora: Cláudia Pio Ferreira
Coorientador: Odair Aparecido Fernandes

1. Biometria. 2. Matemática aplicada. 3. Equações
diferenciais funcionais. 4. Equações diferenciais parciais.
5. Estatística. I. Título.

Sistema de geração automática de fichas catalográficas da Unesp. Biblioteca do
Instituto de Biociências, Botucatu. Dados fornecidos pelo autor(a).

Essa ficha não pode ser modificada.

ATA DA DEFESA PÚBLICA DA TESE DE DOUTORADO DE ANTONE DOS SANTOS BENEDITO, DISCENTE DO PROGRAMA DE PÓS-GRADUAÇÃO EM BIOMETRIA, DO INSTITUTO DE BIOCÊNCIAS - CÂMPUS DE BOTUCATU.

Aos 21 dias do mês de fevereiro do ano de 2020, às 14:00 horas, no(a) LDI III do Departamento de Bioestatística, Biologia Vegetal, Parasitologia e Zoologia, reuniu-se a Comissão Examinadora da Defesa Pública, composta pelos seguintes membros: Profa. Dra. CLAUDIA PIO FERREIRA - Orientador(a) do(a) Departamento de Bioestatística, Biologia Vegetal, Parasitologia e Zoologia / Instituto de Biociências de Botucatu - UNESP, Prof. Dr. RENATO MENDES COUTINHO do(a) Centro de Matemática, Computação e Cognição / Universidade Federal do ABC - UFABC, Prof. Dr. WESLEY AUGUSTO CONDE GODOY do(a) Departamento de Entomologia e Acarologia / ESALQ - USP - Piracicaba/SP, Prof. Dr. JOSÉ BRUNO MALAQUIAS do(a) Departamento de Bioestatística, Biologia Vegetal, Parasitologia e Zoologia / Instituto de Biociências de Botucatu - UNESP, Prof. Dr. PAULO FERNANDO DE ARRUDA MANCERA do(a) Departamento de Bioestatística, Biologia Vegetal, Parasitologia e Zoologia / Instituto de Biociências de Botucatu - UNESP, sob a presidência do primeiro, a fim de proceder a arguição pública da TESE DE DOUTORADO de ANTONE DOS SANTOS BENEDITO, intitulada **MULTI-STAGE POPULATION MODELS APPLIED TO INSECT DYNAMICS**. Após a exposição, o discente foi arguido oralmente pelos membros da Comissão Examinadora, tendo recebido o conceito final: aprovado. Nada mais havendo, foi lavrada a presente ata, que após lida e aprovada, foi assinada pelos membros da Comissão Examinadora.

Profa. Dra. CLAUDIA PIO FERREIRA



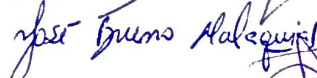
Prof. Dr. RENATO MENDES COUTINHO



Prof. Dr. WESLEY AUGUSTO CONDE GODOY



Prof. Dr. JOSÉ BRUNO MALAQUIAS



Prof. Dr. PAULO FERNANDO DE ARRUDA MANCERA



Acknowledgements

I would like to thank Cláudia Pio Ferreira for her inestimable encouragement and guidance as my advisor, Odair Aparecido Fernandes for all his advice and support as my co-advisor and Mostafa Adimy for sharing his time and knowledge during my stay at Inria Antenne Lyon la Doua, France. I would also like to thank Éllen Rimkevicius Carbognin for her essential laboratorial assistance. Furthermore, I thank my wife, parents and plenty of friends for all their cheer and incentive. Finally, I thank to CAPES (Coordenação de Aperfeiçoamento de Pessoal de Nível Superior – Brasil) - Finance Code 001 for its financial support to my doctoral scholarship both in Brazil and France (PDSE process number: 88881.188834/2018-01).

Abstract

This thesis presents two manuscripts previously sent to publication in scientific journals. In the first manuscript, a delay differential equation model is developed to study the dynamics of two *Aedes aegypti* mosquito populations: infected by the intracellular bacteria *Wolbachia* and non-infected (wild) individuals. All the steady states of the system are determined, namely extinction of both populations, extinction of the infected population and persistence of the non-infected one, and coexistence. Their local stability is analyzed, including Hopf bifurcation, which promotes periodic solutions around the nontrivial equilibrium points. Finally, one investigates the global asymptotic stability of the trivial solution. In the second manuscript, after rearing soybean looper *Chrysodeixis includens* in laboratory conditions, thermal requirements for this insect-pest are estimated, from linear and nonlinear regression models, as well as the intrinsic growth rate. This parameter depends on the life-history traits and can provide a measure of population viability of the species.

Contents

| | Página |
|---|--------|
| 1 INTRODUCTION | 1 |
| 2 MODELING THE DYNAMICS OF <i>WOLBACHIA</i> -INFECTED AND UNINFECTED <i>AEDES AEGYPTI</i> POPULATIONS BY DELAY DIFFERENTIAL EQUATIONS | 5 |
| 3 THERMAL REQUIREMENTS AND POPULATION VIABILITY OF SOYBEAN LOOPER (LEPIDOPTERA: NOCTUIDAE) | 30 |
| 4 CONCLUSIONS AND FURTHER WORK | 50 |
| REFERÊNCIAS BIBLIOGRÁFICAS | 52 |

1 INTRODUCTION

Insect invasions and insect outbreaks have dominated the headlines worldwide for decades. Some of them are important agents of large economic losses and of disease transmission. Numerous efforts have been employed by the scientific and no-scientific community to treat these issues by solving or softening them. Applied mathematics and statistics, often combined, are an relevant support to this purpose, since they allow to understand, describe and evaluate the underlying mechanisms of insect dynamics. Tools like differential equations (deterministics and stochastics), optimization models, regression models, survival analysis, individual-based models, complex networks and many others have been broadly used.

Abiotic factors such as temperature and humidity, influence insects temporal and spatial dynamics both directly and indirectly. The direct influence can be observed through limiting and stimulating the activity of larvae and adults, insect dispersal, insect development rate, insect survival in adverse weather conditions, etc. Indirect influence includes modulation of the environment where the insect lives, such as plant formation and phenology, food quality, number of predators and parasitoids, and activity of entomopathogens (Jaworski & Hilszczański, 2013).

Complex relations among these factors have been gradually understood but not completely explained. For instance, the closer is the environment temperature to the thermal optima, the faster is the insect metabolism leading to greater feeding and mating activities, and the longer is the time seeking places of oviposition. This may increase the chances of dispersing, the frequency of laying eggs, and the probability of colonising a larger number of host plants (Moore & Allard, 2008). The shortening of immature development in higher environment temperatures can

result in reproductive success of many insects since there would be a shorter time of immature exposition to adverse conditions such as low temperature, extremely high or inadequate humidity, predator or parasitoid attacks and entomopathogenic activity. Furthermore, fast-growing may, in addition to shorten the biological life cycle, increase the generation number and outbreak frequency of some species (Netherer & Schopf, 2010).

Therefore, understanding the connection between vital rates and temperature variation is crucial for predicting seasonal fluctuation of insect populations and developing strategies of control. Several empirical linear and nonlinear models of temperature-dependent development rate have been established to estimate the vital thermal requirements from life table data of poikilothermic species obtained at constant temperatures in laboratory (Damos & Savopoulou-Soultani, 2012).

Moreover, developmental and other life-cycle traits models might be incorporated in mathematical models to predict seasonal insect abundance and outbreak timing in field. Among them, delay differential equation (DDE) models have shown to be appropriate to describe the dynamics of species with stage-structured life cycles, and they also allow changing the stage duration driven by biotic or abiotic factors.

Besides their exclusive property of capturing delayed feedback, DDE models are only slightly more complex than ordinary differential equation (ODE) to simulate numerically and simpler as for mathematical analysis compared to partial differential equation (PDE) models (Kim et al., 2009). DDE modeling has been used in many distinct areas such as medicine, engineering and industry, ecology, genetics and so on for the most variable applications, e.g. cardiovascular system (Ottesen, 1997), teleoperation problems (Kruszewski et al., 2014), gene regulatory networks (Ahsen et al., 2014), glucose-insulin systems for diabetes patients (Palumbo et al., 2014), neural networks (Orosz, 2014), cell population dynamics in cancer treatment (Avila et al., 2014) among others.

In this context, the current thesis presents two manuscripts already

submitted to scientific journals related to both aforementioned classes of biological problem. Two different insects were chosen: (i) *Aedes aegypti* and (ii) *Chrysodeixis includens*. The first one is a known vector of many vector-borne diseases, such as dengue, Zika, Chikungunya, and yellow fever, causing millions of human deaths every year; and the second one is the main plusine pest in the Americas, for the sake of damage caused to soybean and also to many other crop species across a broad geographical range.

The first manuscript introduces a new DDE model, reducible to a Nicholson-type delay system under some parametric conditions, to study the colonization and persistence of *Wolbachia*-transinfected *Aedes aegypti* into environments wherein an uninfected wild mosquito population is already settled. This model is derived by the method of characteristics from a previous PDE model. A broad theoretical analysis is held including positiveness, boundedness, and uniqueness of solutions, local stability of steady states, Hopf bifurcation and the global stability of the trivial steady state given by the extinction of both populations. The results gathered in this work can lead to further study about the influence of abiotic factors on the dynamics of these populations, so long as they cause change in the immature development time, e.g. the temperature.

In the second manuscript, the thermal requirements of soybean looper *Chrysodeixis includens*, namely lower and upper temperature thresholds and optimal temperature for immature stages, are unprecedentedly obtained through linear and nonlinear temperature-driven models fitted to laboratory data. The latter were also used to evaluate the population viability under different temperatures, for which the intrinsic growth rate was calculated as a function of the life-history traits. Hopefully, the results achieved here may be used to forecast accurately the occurrence of the different stages of *C. includens* in field and help optimize the efforts of controlling this insect-pest. In this sense, a new study addressing the modeling of *C. includens* life cycle by DDE equations considering the temperature-dependence of the model parameters is in progress. This survey will put together the knowledge acquired in

the two previous works.

I would like to highlight two periods of my doctorate: (i) supported by CAPES (PDSE process number: 88881.188834/2018-01), a sandwich period from late August 2018 to early March 2019 was done at Inria (Institut National de Recherche en Informatique et en Automatique), Lyon, France. My supervisor abroad was Mostafa Adimy, whose teaching and guidance were important in consolidating the theoretical knowledge about DDE systems; (ii) laboratorial data of *C. includens* were collected from June 2018 to late August 2018 at School of Agricultural and Veterinary Sciences, São Paulo State University (UNESP), Jaboticabal-SP, Brazil, supervised by Odair Aparecido Fernandes. Records of development time, longevity, mortality and fecundity at different temperatures, so far missing in the literature for this species, were performed. This laboratory work has been a wealth of experience in terms of learning and professional formation.

MODELING THE DYNAMICS OF *WOLBACHIA*-INFECTED AND UNINFECTED *Aedes aegypti* POPULATIONS BY DELAY DIFFERENTIAL EQUATIONS

A. S. BENEDITO¹, C. P. FERREIRA¹ AND M. ADIMY²

Abstract. Starting from an age structured partial differential model, which takes into account the mosquito life cycle and the main features of the *Wolbachia*-infection, we derive a delay differential model by using the method of characteristics to study the colonization and persistence of the *Wolbachia*-transfected *Aedes aegypti* mosquito in an environment in which the uninfected wild mosquito population is already established. Under some conditions, the model can be reduced to a Nicholson-type delay differential system, where the delay represents the duration of mosquito immature phase that comprises egg, larva and pupa. In addition to mortality and oviposition rates characteristic of the life cycle of the mosquito, other biological features such as cytoplasmic incompatibility, bacterial inheritance and sex ratio deviation are considered in the model. There exist three equilibriums: the extinction of both populations, the extinction of *Wolbachia*-infected population and persistence of uninfected one, and their coexistence. Analytical conditions of existence for each equilibrium are provided and biologically interpreted. It is shown that the increase of the delay can promote, through Hopf bifurcation, stability switch towards instability for the nonzero equilibriums. Overall, when the delay increases and crosses predetermined thresholds, the populations go to extinction.

...

INTRODUCTION

Aedes aegypti is a widespread human blood-feeding mosquito responsible for the transmission of several arboviruses including Dengue, Yellow fever, Zika, Murray Valley, La Crosse, Chikungunya and Rift Valley fever. For most of these diseases an efficient vaccine is not available and the reduction of mosquito population is still the only way to prevent epidemics [17]. The traditional approach to diminishing the mosquito population includes the reduction of breeding sites and the use of larvicides and pesticides for adults. In general, mechanical control and the application of larvicides are carried out before the period favorable to the proliferation of mosquitoes, while pesticides for adults are applied during epidemics when the number of infected humans is high [41]. Environmentally-friendly techniques include the use of sterile males (SIT) [8, 16] and *Wolbachia*-infected mosquitoes [7, 15]. While the first one focus on the reduction of mosquito population to halt disease transmission, the second one aims to replace the wild population for an infected one that is not able to transmit the virus. Both require the release of a large number of mosquitoes, hence a combination between traditional and new technologies are encouraged [33].

Keywords and phrases. Age structured partial differential system, delay differential system, local and global asymptotic stability, Hopf bifurcation

¹ São Paulo State University (UNESP), Institute of Biosciences, 18618-689 Botucatu, SP, Brazil; e-mail: antone.santos@unesp.br & claudia.pio@unesp.br

² Inria, Université de Lyon, Université Lyon 1, 69200 Villeurbanne, France; e-mail: mostafa.adimy@inria.fr

The intracellular bacteria of the genus *Wolbachia* manipulates host reproductive systems to increase its transmission by inducing parthenogenesis, feminization, male-killing or cytoplasmic incompatibility (CI) [2, 37]. Additionally, the bacteria is transmitted vertically from mother to its offspring. Put together, these characteristics confer a fitness advantage over uninfected population that can drive the *Wolbachia*-infected population to fixation [20, 24]. The same is not true for the SIT, since the mating with sterile mosquitoes does not produce viable offspring; they must therefore be introduced periodically.

In field, the *Wolbachia* strains that have been used in releases come from *Drosophila melanogaster*, wMel and wMelPop, and from *Aedes albipicus*, wAlbB. Artificial infections with new strains of bacteria still be done in laboratory in order to increase technique factibility. This is because recent research has shown that biotics and abiotics factors can influence *Wolbachia* densities and its distribution in mosquito tissue, and if the thresholds related to heritability and cytoplasmic incompatibility cannot be achieved the technique efficacy is lost [9, 35, 37]. The thermal sensitivity of *Wolbachia*-infection is variable and can differ considerably between host species and strains. High temperatures might reduce its density in hosts, weaken the reproductive effects induced by *Wolbachia*-infection and even eradicate *Wolbachia* completely. In *Ae. aegypti*, the wAlbB infection type is more stable than wMel and wMelPop at high temperatures [35].

Moreover, for poikilothermic species such as the *Aedes aegypti* mosquito, the body temperature depends on external factors and has strong effects over its entomological parameters and behavior. The lower and upper developmental threshold are 16°C and 34°C, being the development time shorter at higher temperatures [34]. Also, the survival of immatures and adults may be negatively influenced by large diurnal temperature range since their mortality rates present U-shaped forms [42]. The oviposition rate in turn increases quasi-linearly with temperature increasing [42]. Both flight activity and mating rate were detected to increase with temperature ranging from 18°C to 31°C [11]. Moreover, it was found that the length of the gonotrophic cycle was reduced with increasing mean temperatures. Besides, wing beat frequency, blood-feeding, biting activity, host seek among other behavior characters are significantly affected by temperature variation [34].

Several mathematical models have been addressing the use of *Wolbachia* infected mosquitoes to control dengue (and other viruses) transmission, because the presence of the bacteria reduces vector competence [28, 31, 32]. In [14], a sex-structured model taking into account cytoplasmic incompatibility, male killing, incomplete maternal transmission, and different mortality rates for uninfected/infected population was developed. The boundedness of population was provided by considering competition among females for nesting places which give an upper limit for egg-laying rate. The ordinary differential model was studied analytically, and it was shown that the steady state where the *Wolbachia*-infected individuals dominate the population is possible when the maternal transmission is complete and cytoplasmic incompatibility is high. Coexistence of *Wolbachia*-infected and uninfected mosquito and *Wolbachia*-free equilibrium are found for a large set of relevant biological parameters. By considering that density-dependent death rate controls the exponential growth of populations, [27] showed that only when the initial level of infection (given by the percentage of *Wolbachia*-infected population), breaks some critical thresholds that the infection takes off from the population (i.e. the threshold for invasion is achieved). In [31], the aquatic stage was also included and population boundedness was guaranteed by considering a logistic carrying capacity on this phase. It was shown that *Wolbachia*-infected mosquitoes always dominate the population provided they persist. The same approach was done in [29] and the existence of a minimum infection frequency above which *Wolbachia* could spread into the whole population of mosquitoes was explored. All of these mathematical models used ordinary differential equations to model the temporal dynamics of the mosquito population.

In turn, partial differential equations (PDE) are much less explored. Some studies such as [19, 21] present reaction-diffusion models for the *Wolbachia*-infected and uninfected populations. They concluded that there is no spatial influence on the stability criteria for the steady states. Moreover, [21] focused on determining the threshold for invasion of the wild population by the *Wolbachia*-infected one. Further, [13] compares the stability results of the equilibriums obtained for an age-structured (PDE) with the one of an unstructured (ODE) model. For simplicity, two asexual population were considered, uninfected and *Wolbachia*-infected one.

Finally, rarer is the use of delay differential equations (DDE) for such problem. In [22], a DDE phase-structured model (larva and adult populations) evaluated the suppression of the wild population of *Aedes* mosquitoes by releasing a continuous constant number of *Wolbachia*-infected male. This is modeled by changing the growing rate of the population. The model considered two delays, one representing the average time from adult emergence to the hatching of the first larval stage (which determines larva population growth), and the other the average time from the first larval stage to adult emergence (which models adult population growth). Also, a strong density-dependent death rate was considered in the larval stage. They concluded that the delays do not impact population suppression. A modification of this model was proposed in [23] to compare two opposite phenomena which are the decrease on mating competitiveness of the released males relative to the wild males and the fitness advantage given by the cytoplasmic incompatibility probability to the *Wolbachia*-infected population over the wild one. The model considers only adult population and the delay gives the contribution of the last generation to the growth of the new population. They showed that CI plays a more important role in the suppression of *Aedes* population.

Then, starting from an age structured PDE model which considers the mosquito entomological parameters and also biological features associated to *Wolbachia* infection, a new two-population DDE model is obtained and carefully assessed. Analytical results such as positiveness, boundedness, and uniqueness of solutions are provided. Further, thresholds for existence and stability of the steady states were obtained and interpreted in the context of population fitness. The role performed by the delay on the insect temporal dynamics can help to understand the effect of changing abiotic factors such as temperature on the long-run behavior of these populations. The model appears for the first time in [15] where numerical results concerning population dynamics are explored.

1. AGE STRUCTURED PARTIAL DIFFERENTIAL MODEL

Let w and u be *Wolbachia*-infected and uninfected mosquito status. We denote $f_j := f_j(t, a)$ with $j \in \{w, u\}$ the female population density of mosquito, $a \in [0, \tau)$ the physiological age of the immature phase including egg, larva and pupa, $a \geq \tau$ the physiological age of the mature phase (fertile adults), t the calendar time, μ_w and μ_u the adult mortality rates, and μ the immature mortality rate. We assume that the parameters τ and μ are the same for infected and uninfected mosquitoes [31]. The temporal evolution of mosquito population satisfies the following age-structured Lotka-McKendrick system

$$\frac{\partial f_j}{\partial t} + \frac{\partial f_j}{\partial a} = -\kappa_j(a)f_j, \quad j \in \{w, u\}, \quad (1)$$

where

$$\kappa_j(a) = \begin{cases} \mu, & a \in [0, \tau), \\ \mu_j, & a \geq \tau. \end{cases}$$

The *Wolbachia* bacteria is transmitted from mother to its offspring with probability $\xi_w \in (0, 1)$. Thus, with probability

$$\xi_u := 1 - \xi_w \quad (2)$$

an infected female can produce uninfected offspring. The mating probability between an uninfected female and an infected male is denoted by $\nu \in (0, 1)$ and the probability of cytoplasmic incompatibility occurrence is $q \in (0, 1)$. This means that the fraction of matings between uninfected females and infected males that produce viable eggs is given by $1 - q\nu$. The average birth rates are $\phi_w > 0$, $\phi_u > 0$ with the average percentage of female births $r_w, r_u \in (0, 1)$. We denote by

$$F_j(t) = \int_{\tau}^{+\infty} f_j(t, a) da, \quad j \in \{w, u\}, \quad (3)$$

4

the total population of infected and uninfected adult females, respectively. Therefore, the newborn individuals introduced into the population are given at $a = 0$ by

$$\begin{aligned} f_w(t, 0) &= \xi_w r_w \phi_w F_w(t) G(F_w(t), F_u(t)), \\ f_u(t, 0) &= [(1 - q\nu) r_u \phi_u F_u(t) + \xi_u r_w \phi_w F_w(t)] G(F_w(t), F_u(t)), \end{aligned} \quad (4)$$

where $G(X, Y) = e^{-\alpha(E_w X + E_u Y)^\eta}$ measures competition among individuals. More precisely, to take into account the competition between mosquitoes for oviposition sites, the number of eggs per female is multiplied by the density-dependent factor $G(F_w(t), F_u(t))$. The parameters $\alpha > 0$ and $\eta > 0$ are, respectively, the environmental carrying capacity and the measurement of how rapidly it is achieved [12]. The parameters E_w and E_u take into account the different behaviors between infected and uninfected females. In addition, the populations are assumed to satisfy

$$\lim_{a \rightarrow +\infty} f_j(t, a) = 0, \quad j \in \{w, u\}, \quad t > 0. \quad (5)$$

The initial age-distribution $f_j(0, a)$, $j \in \{w, u\}$, is assumed to be known. Finally, as we are assuming that the mating between male and female is given by a constant parameter ν , we do not need to explicitly model the male population, and we will omit it from the analysis.

2. REDUCTION TO A DELAY DIFFERENTIAL SYSTEM

Henceforth, we reduce the system (1)-(5) to delay differential equations. We denote by

$$F_j^i(t) = \int_0^\tau f_j(t, a) da, \quad j \in \{w, u\}, \quad (6)$$

the total population of immature females, *Wolbachia*-infected and uninfected, respectively. By integrating the system (1) over the age variable from 0 to τ and from τ to $+\infty$, respectively, we get for $j \in \{w, u\}$,

$$\begin{cases} \frac{d}{dt} F_j^i(t) = -\mu F_j^i(t) + f_j(t, 0) - f_j(t, \tau), \\ \frac{d}{dt} F_j(t) = -\mu_j F_j(t) + f_j(t, \tau), \end{cases}$$

where F_j is given by (3) and F_j^i by (6). On the other hand, the method of characteristics (see [36]) implies that

$$f_j(t, \tau) = \begin{cases} f_j(0, \tau - t) e^{-\mu t}, & 0 \leq t \leq \tau, \\ f_j(t - \tau, 0) e^{-\mu \tau}, & t > \tau. \end{cases}$$

As we are interested on the asymptotic behavior of the population, we can assume that t is large enough such that $t > \tau$. Then,

$$f_j(t, \tau) = f_j(t - \tau, 0) e^{-\mu \tau}, \quad j \in \{w, u\}.$$

By adding the boundary conditions (4), we get the following delay differential system

$$\left\{ \begin{array}{l} \frac{d}{dt} F_w^i(t) = -\mu F_w^i(t) + \xi_w r_w \phi_w F_w(t) G(F_w(t), F_u(t)) \\ \quad - e^{-\mu\tau} \xi_w r_w \phi_w F_w(t-\tau) G(F_w(t-\tau), F_u(t-\tau)), \\ \frac{d}{dt} F_w(t) = -\mu_w F_w(t) + e^{-\mu\tau} \xi_w r_w \phi_w G(F_w(t-\tau), F_u(t-\tau)) F_w(t-\tau), \\ \frac{d}{dt} F_u^i(t) = -\mu F_u^i(t) + [(1-q\nu)r_u \phi_u F_u(t) + (1-\xi)r_w \phi_w F_w(t)] \\ \quad \times G(F_w(t), F_u(t)) \\ \quad - e^{-\mu\tau} [(1-q\nu)r_u \phi_u F_u(t-\tau) + \xi_u r_w \phi_w F_w(t-\tau)] \\ \quad \times G(F_w(t-\tau), F_u(t-\tau)), \\ \frac{d}{dt} F_u(t) = -\mu_u F_u(t) + e^{-\mu\tau} [(1-q\nu)r_u \phi_u F_u(t-\tau) + \xi_u r_w \phi_w F_w(t-\tau)] \\ \quad \times G(F_w(t-\tau), F_u(t-\tau)), \end{array} \right.$$

where F_j^i , F_j , $j \in \{w, u\}$, are the total population of immature and adult females, *Wolbachia*-infected and uninfected, respectively. We can see that the equations of mature population F_j are independent on the equations of immature one F_j^i . Then, we will omit the system of F_j^i and concentrate only on F_j . Remembering that the nonlinear function G is given by

$$G(X, Y) = e^{-\alpha(E_w X + E_u Y)^n},$$

we carry out the transformations

$$w(t) := \alpha^{\frac{1}{n}} E_w F_w(t), \quad u(t) := \alpha^{\frac{1}{n}} E_u F_u(t),$$

and we define the new parameters

$$P_w := \xi_w r_w \phi_w, \quad P_u := (1-q\nu)r_u \phi_u \quad \text{and} \quad P_{wu} := \xi_u r_w \phi_w; \quad (7)$$

respectively, the number of infected eggs per time per infected individual that will hatch, the number of uninfected eggs per time per uninfected individual that will hatch, and the number of uninfected eggs per time per infected individual that will hatch.

Then, the model can be reduced, for $t > \tau$, to

$$\left\{ \begin{array}{l} \frac{d}{dt} w(t) = -\mu_w w(t) + e^{-\mu\tau} P_w w(t-\tau) e^{-(w(t-\tau)+u(t-\tau))^n}, \\ \frac{d}{dt} u(t) = -\mu_u u(t) + e^{-\mu\tau} [P_u u(t-\tau) + P_{wu} w(t-\tau)] e^{-(w(t-\tau)+u(t-\tau))^n}, \end{array} \right. \quad (8)$$

with initial conditions given by

$$(w(t), u(t)) = (\bar{\Psi}_w(t), \bar{\Psi}_u(t)), \quad t \in [0, \tau]. \quad (9)$$

We make a translation in time so as to define the system (8) on the interval $[0, +\infty)$ and the initial conditions (9) on the interval $[-\tau, 0]$.

Remark 2.1. If we consider the case

$$\mu_w = \mu_u := \delta, \quad P_w + P_{wu} = P_u \quad \text{and} \quad \eta = 1,$$

6

then, we obtain the famous Nicholson's blowflies equation

$$N'(t) = -\delta N(t) + pN(t-\tau)e^{-N(t-\tau)}, \quad (10)$$

where $N = w + u$ and $p = P_u e^{-\mu\tau}$. The equation (10) has been extensively studied in the literature [5, 6, 10]. The main results on equation (10) deal with the global attractivity of the positive steady state and the existence of oscillatory solutions (see [6]).

3. POSITIVITY AND BOUNDEDNESS OF SOLUTIONS

The positivity and boundedness of solutions are important in biological models. We first establish an existence and uniqueness theorem about the positive solution for the nonlinear delay differential system (8)-(9).

Theorem 3.1. *For any nonnegative continuous initial function $(\bar{\Psi}_w, \bar{\Psi}_u)$ on $[-\tau, 0]$, there is a unique nonnegative global solution (w, u) of the problem (8)-(9). Furthermore, $t \mapsto (w(t), u(t))$ is such that $w(t) > 0$, $u(t) > 0$, for $t \geq 0$ provided that $\bar{\Psi}_w(t) \geq 0$, $\bar{\Psi}_u(t) \geq 0$, for all $t \in [-\tau, 0)$ and $\bar{\Psi}_w(0) > 0$, $\bar{\Psi}_u(0) > 0$.*

Proof. It follows from the standard existence theorem [26], that there exists a unique local solution (w, u) of the problem (8)-(9), defined on an interval $[-\tau, t_0)$, $t_0 > 0$. By steps, suppose that $t \in [0, \tau]$. Then, $t - \tau \in [-\tau, 0]$, and using the variation of constants formula for the system (8)-(9), we obtain for $t \in [0, \tau]$,

$$w(t) = \bar{\Psi}_w(0)e^{-\mu_w t} + P_w e^{-\mu\tau} e^{-\mu_w t} \int_0^t \bar{\Psi}_w(s-\tau) e^{-(\bar{\Psi}_w(s-\tau) + \bar{\Psi}_u(s-\tau))^\eta} e^{\mu_w s} ds \quad (11)$$

and

$$u(t) = \bar{\Psi}_u(0)e^{-\mu_u t} + e^{-\mu\tau} e^{-\mu_u t} \int_0^t [P_u \bar{\Psi}_u(s-\tau) + P_{wu} \bar{\Psi}_w(s-\tau)] \times e^{-(\bar{\Psi}_w(s-\tau) + \bar{\Psi}_u(s-\tau))^\eta} e^{\mu_u s} ds. \quad (12)$$

Then, for a nonnegative initial condition $(\bar{\Psi}_w, \bar{\Psi}_u)$ on $[-\tau, 0]$, we have a nonnegative solution (w, u) on $[0, \tau]$. Through the method of steps, we have $w(t) \geq 0$, $u(t) \geq 0$ on $[\tau, 2\tau]$, $[2\tau, 3\tau]$, and so on. Thus, $w(t) \geq 0$, $u(t) \geq 0$ for all $t \in [0, t_0)$. We suppose by contradiction that (w, u) exists only on an interval $[-\tau, t_0)$ with $0 < t_0 < \infty$. Let

$$y(t) = w(t) + u(t), \quad t \in [-\tau, t_0).$$

Then, $\lim_{t \rightarrow t_0^-} y(t) = +\infty$. We define the constant $M = e^{-\mu\tau} \max\{P_u, P_w + P_{wu}\}$ and the function $g(x) = x e^{-x^\eta}$. We have

$$\max_{x \geq 0} g(x) = g\left(\left(\frac{1}{\eta}\right)^{\frac{1}{\eta}}\right) = \left(\frac{1}{\eta e}\right)^{\frac{1}{\eta}}.$$

Then, from the system (8), we can write the following estimation

$$\begin{aligned} \frac{d}{dt} y(t) &= -\mu_w w(t) - \mu_u u(t) \\ &\quad + e^{-\mu\tau} [P_u u(t-\tau) + (P_w + P_{wu})w(t-\tau)] e^{-(w(t-\tau) + u(t-\tau))^\eta}, \\ &\leq -\min\{\mu_w, \mu_u\} y(t) + M \left(\frac{1}{\eta e}\right)^{\frac{1}{\eta}}. \end{aligned}$$

Hence, y is bounded on the interval $[-\tau, t_0)$. This gives a contradiction and proves that the problem (8)-(9) has a global solution on the interval $[-\tau, +\infty)$. Now, we assume that $\bar{\Psi}_w, \bar{\Psi}_u \geq 0$ on $[-\tau, 0)$ and $\bar{\Psi}_w(0), \bar{\Psi}_u(0) > 0$. Using the variation of constants formulas (11)-(12), we get $w(t), u(t) > 0$, for all $t \in [0, \tau]$. By steps, we prove that $w(t), u(t) > 0$, for all $t \geq 0$. \square

Proposition 3.2. *The solution (w, u) of the system (8)-(9) is bounded on the interval $[0, +\infty)$, with*

$$\limsup_{t \rightarrow +\infty} w(t) \leq \frac{P_w e^{-\mu\tau}}{\mu_w} \left(\frac{1}{\eta e} \right)^{\frac{1}{\eta}}, \quad \limsup_{t \rightarrow +\infty} u(t) \leq \frac{(P_u + P_{wu}) e^{-\mu\tau}}{\mu_u} \left(\frac{1}{\eta e} \right)^{\frac{1}{\eta}}.$$

Proof. Let $f(x) = P_w e^{-\mu\tau} g(x)$, for $x \geq 0$. We have

$$\max_{x \geq 0} f(x) = P_w e^{-\mu\tau} g \left(\left(\frac{1}{\eta} \right)^{\frac{1}{\eta}} \right) = P_w e^{-\mu\tau} \left(\frac{1}{\eta e} \right)^{\frac{1}{\eta}}.$$

Then, from (8) we obtain

$$\frac{d}{dt} w(t) \leq -\mu_w w(t) + P_w e^{-\mu\tau} w(t - \tau) e^{-w(t-\tau)^\eta} \leq -\mu_w w(t) + P_w e^{-\mu\tau} \left(\frac{1}{\eta e} \right)^{\frac{1}{\eta}}.$$

The last inequality implies that

$$w(t) \leq \frac{P_w e^{-\mu\tau}}{\mu_w} \left(\frac{1}{\eta e} \right)^{\frac{1}{\eta}} [1 - e^{-\mu_w t}] + e^{-\mu_w t} w(0).$$

Then,

$$\limsup_{t \rightarrow +\infty} w(t) \leq \frac{P_w e^{-\mu\tau}}{\mu_w} \left(\frac{1}{\eta e} \right)^{\frac{1}{\eta}}.$$

This completes the proof of the boundedness of $w(t)$.

By using the same argument, we can write

$$\frac{d}{dt} u(t) \leq -\mu_u u(t) + (P_u + P_{wu}) e^{-\mu\tau} \left(\frac{1}{\eta e} \right)^{\frac{1}{\eta}}.$$

This implies that

$$u(t) \leq \frac{(P_u + P_{wu}) e^{-\mu\tau}}{\mu_u} \left(\frac{1}{\eta e} \right)^{\frac{1}{\eta}} [1 - e^{-\mu_u t}] + e^{-\mu_u t} u(0).$$

Then, we conclude that

$$\limsup_{t \rightarrow +\infty} u(t) \leq \frac{(P_u + P_{wu}) e^{-\mu\tau}}{\mu_u} \left(\frac{1}{\eta e} \right)^{\frac{1}{\eta}}.$$

□

4. EXISTENCE OF STEADY STATES

Let (w^*, u^*) be a steady state of the system (8). Then,

$$\begin{cases} P_w e^{-\mu\tau} w^* e^{-(w^*+u^*)^\eta} - \mu_w w^* & = 0, \\ (P_u u^* + P_{wu} w^*) e^{-\mu\tau} e^{-(w^*+u^*)^\eta} - \mu_u u^* & = 0. \end{cases} \quad (13)$$

8

Defining

$$\delta_w := \frac{P_w}{\mu_w} = \frac{\xi_w r_w \phi_w}{\mu_w}, \quad \delta_u := \frac{P_u}{\mu_u} = \frac{(1-q\nu)r_u \phi_u}{\mu_u} \quad (14)$$

and

$$\delta_{wu} := \frac{P_{wu}}{\mu_u} = \frac{\xi_u r_w \phi_w}{\mu_u}, \quad (15)$$

the system (13) can be rewritten as

$$\begin{cases} \delta_w e^{-\mu\tau} w^* e^{-(w^*+u^*)^\eta} - w^* & = 0, \\ (\delta_u u^* + \delta_{wu} w^*) e^{-\mu\tau} e^{-(w^*+u^*)^\eta} - u^* & = 0, \end{cases}$$

and we obtain three solutions \mathbf{S}_0 , \mathbf{S}_u and \mathbf{S}_{wu} of this system which are:

(i) Extinction of both populations (trivial equilibrium)

$$\mathbf{S}_0 = (0, 0); \quad (16)$$

(ii) Extinction of infected population and persistence of uninfected one

$$\mathbf{S}_u = \left(0, (\ln R_u)^{\frac{1}{\eta}}\right), \quad \text{with } R_u = \delta_u e^{-\mu\tau}; \quad (17)$$

(iii) Persistence of both populations (coexistence of infected and uninfected mosquitoes)

$$\begin{aligned} \mathbf{S}_{wu} &= \left((\ln R_w)^{\frac{1}{\eta}} (1 - \beta_{wu}), (\ln R_w)^{\frac{1}{\eta}} \beta_{wu} \right), \\ \text{with } R_w &= \delta_w e^{-\mu\tau} \quad \text{and} \quad \beta_{wu} = \frac{\delta_{wu}}{\delta_w - \delta_u + \delta_{wu}}. \end{aligned} \quad (18)$$

By examining the components of the steady states, we can deduce the following existence conditions.

- Proposition 4.1.** (a) \mathbf{S}_0 always exists;
 (b) \mathbf{S}_u exists if and only if $R_u > 1$;
 (c) \mathbf{S}_{wu} exists if and only if $R_w > \max\{1, R_u\}$.

In terms of the original parameters, we have

$$R_w = \frac{\xi_w r_w \phi_w}{\mu_w} e^{-\mu\tau} \quad \text{and} \quad R_u = \frac{(1-q\nu)r_u \phi_u}{\mu_u} e^{-\mu\tau}.$$

The two dimensionless parameters R_w and R_u are, respectively, the mean number of female infected offspring produced by a *Wolbachia*-infected female mosquito during her whole life, and the mean number of female uninfected offspring produced by an uninfected female mosquito during her whole life.

As we are interested on the relationship between temperature variation (that affects strongly the maturation time τ) and population dynamics of both *Wolbachia*-infected and uninfected mosquitoes, we have to study the existence of the steady states in terms of the delay τ . We consider the following thresholds of the maturation time

$$\tau_j = \frac{1}{\mu} \ln(\delta_j), \quad j \in \{w, u\}. \quad (19)$$

In fact, $\tau_j \in \mathbb{R}$ and we have:

- (1) $\tau_j \geq 0$ if and only if $\delta_j \geq 1$, and
- (2) $\tau_j < 0$ if and only if $0 < \delta_j < 1$.

In terms of the delay, we obtain the following result.

Proposition 4.2. (1) \mathbf{S}_u exists if and only if

$$0 \leq \tau < \tau_u.$$

(2) \mathbf{S}_{wu} exists if and only if

$$0 \leq \tau < \tau_w \quad \text{and} \quad \tau_u < \tau_w.$$

We remark that the steady states \mathbf{S}_u and \mathbf{S}_{wu} exist in the same time if and only if

$$0 \leq \tau < \tau_u \quad \text{and} \quad \tau_u < \tau_w.$$

In summary, we can distinguish four situations.

Proposition 4.3. (i) Assume that $0 < \delta_u \leq 1$ and $0 < \delta_w \leq 1$ (which is equivalent to $\tau_u \leq 0$ and $\tau_w \leq 0$). Then, for all $\tau \geq 0$, \mathbf{S}_0 is the only steady state.

(ii) Assume that $\tau_u > 0$ and $\tau_w \leq \tau_u$. Then,

(a) if $0 \leq \tau < \tau_u$, there are two steady states \mathbf{S}_0 and \mathbf{S}_u , with

$$\lim_{\tau \rightarrow \tau_u} \mathbf{S}_u = \mathbf{S}_0;$$

(b) if $\tau \geq \tau_u$, \mathbf{S}_0 is the only steady state.

(iii) Assume that $\tau_u \leq 0 < \tau_w$, ($\tau_u \leq 0$ means $0 < \delta_u \leq 1$). Then,

(a) if $0 \leq \tau < \tau_w$, there are two steady states \mathbf{S}_0 and \mathbf{S}_{wu} , with

$$\lim_{\tau \rightarrow \tau_w} \mathbf{S}_{wu} = \mathbf{S}_0;$$

(b) if $\tau \geq \tau_w$, \mathbf{S}_0 is the only steady state.

(iv) Assume that $0 < \tau_u < \tau_w$. Then,

(a) if $0 \leq \tau < \tau_u$, there are three steady states \mathbf{S}_0 , \mathbf{S}_u and \mathbf{S}_{wu} , with

$$\lim_{\tau \rightarrow \tau_u} \mathbf{S}_u = \mathbf{S}_0;$$

(b) if $\tau_u \leq \tau < \tau_w$, there are two steady states \mathbf{S}_0 and \mathbf{S}_{wu} , with

$$\lim_{\tau \rightarrow \tau_w} \mathbf{S}_{wu} = \mathbf{S}_0;$$

(c) if $\tau \geq \tau_w$, \mathbf{S}_0 is the only steady state.

Figure 1 summarizes the results obtained in Proposition 4.3. The different scenarios correspond to the three parameter sets shown in Table 1. For each τ the corresponding steady state was obtained from (17) or (18). The panel (a) corresponds to case (ii), the panel (b) to case (iii), and the panel (c) to case (iv).

5. STABILITY ANALYSIS OF THE STEADY STATES

5.1. Local asymptotic stability of the trivial steady state \mathbf{S}_0

We conclude from the four scenarios of Proposition 4.3, that the trivial steady state is the only equilibrium if and only if

$$\tau > \max\{0, \tau_u, \tau_w\}. \quad (20)$$

We prove in Theorem 5.2 that the local asymptotic stability of the trivial steady state \mathbf{S}_0 is given by the condition (20). We will need the following useful lemma.

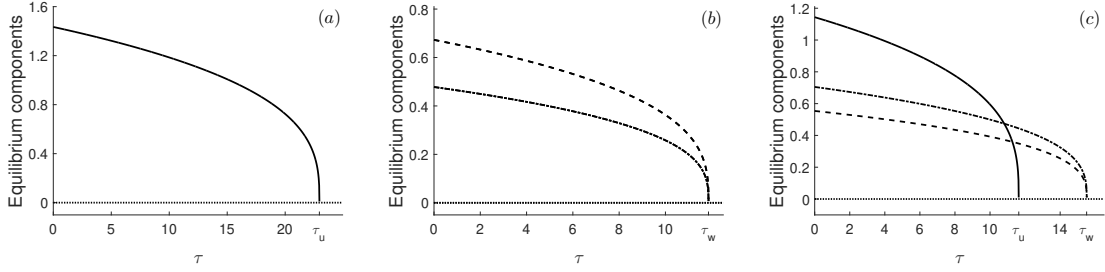


FIGURE 1. Components X and Y of the steady states $\mathbf{S}_j = (X, Y)$, with $\mathbf{j} = \{\mathbf{0}, \mathbf{u}, \mathbf{wu}\}$ versus the delay τ . The parameter sets used in the simulations are given in Table 1, and in all cases $\eta = 3.0$. In (a), we plotted case (ii) in which $\tau_u > 0$ and $\tau_w \leq \tau_u$. Then, if $0 \leq \tau < \tau_u$, there are two steady states \mathbf{S}_0 and \mathbf{S}_u , and if $\tau \geq \tau_u$, \mathbf{S}_0 is the only steady state. In (b), we plotted case (iii) in which $\tau_u \leq 0 < \tau_w$. Then, if $0 \leq \tau < \tau_w$ there are two steady states \mathbf{S}_0 and \mathbf{S}_{wu} , and if $\tau \geq \tau_w$, \mathbf{S}_0 is the only steady state. In (c), we plotted case (iv) in which $0 < \tau_u < \tau_w$. Then, if $0 \leq \tau < \tau_u$, there are three steady states \mathbf{S}_0 , \mathbf{S}_u and \mathbf{S}_{wu} , if $\tau_u \leq \tau < \tau_w$, there are two steady states \mathbf{S}_0 and \mathbf{S}_{wu} , and if $\tau \geq \tau_w$, \mathbf{S}_0 is the only steady state. In all panels \mathbf{S}_0 component Y appears as a dotted line, \mathbf{S}_u component Y appears as a solid, and \mathbf{S}_{wu} component X and Y appear, respectively, as a dot-dashed and dashed line.

TABLE 1. Parameters sets used in all Figures [1, 3, 30, 31, 38, 39, 40, 43].

| Parameter | Value | | | Range [units] |
|---------------|-------------|-------------|-------------|---|
| | case (ii) | case (iii) | case (iv) | |
| q | 0.3 | 0.8 | 0.7 | (0,1) |
| ν | 0.3 | 0.8 | 0.7 | [0,1] |
| ϕ_u | 3.0 | 1.25 | 1.25 | (0.35,11.2) [per day per female] |
| ϕ_w | $2.1\phi_u$ | $2.1\phi_u$ | $2.1\phi_u$ | (0.10,11.0) [per day per female] |
| r_u | 0.5 | 0.5 | 0.5 | (0,1) |
| r_w | 0.5 | 0.5 | 0.5 | (0,1) |
| μ_u | 1/14 | 1/4 | 1/14 | (1/4,1/37) [per day] |
| μ_w | 1/7 | 1/7 | 1/7 | (1/4,1/32) [per day] |
| μ | 1/7.78 | 1/7.78 | 1/7.78 | (1/7.5,1/30) [per day] |
| ξ_w | 0.8 | 0.5 | 0.8 | (0,1) |
| ξ_u | 0.2 | 0.5 | 0.2 | calculated by (2) |
| P_u | 1.37 | 0.22 | 0.32 | calculated by (7) [number of eggs per day per female] |
| P_w | 2.52 | 0.65 | 1.05 | calculated by (7) [number of eggs per day per female] |
| P_{wu} | 0.63 | 0.65 | 0.26 | calculated by (7) [number of eggs per day per female] |
| δ_u | 19.11 | 0.9 | 4.46 | calculated by (14) [number of eggs per female] |
| δ_w | 17.64 | 4.59 | 7.35 | calculated by (14) [number of eggs per female] |
| δ_{wu} | 8.82 | 2.63 | 3.67 | calculated by (14) [number of eggs per female] |
| β_{wu} | 1.2 | 0.41 | 0.56 | calculated by (18) |
| τ_u | 22.95 | -0.81 | 11.64 | calculated by (19) [days] |
| τ_w | 22.33 | 11.86 | 15.52 | calculated by (19)[days] |

Lemma 5.1. [Theorem A.5 in [26], p. 416, see also [18]] All roots of the algebraic equation

$$\lambda + a + be^{-\lambda\tau} = 0,$$

have negative real parts if and only if

- (i) $a\tau > -1$,
- (ii) $a + b > 0$,
- (iii) $b < \zeta \sin \zeta - a\tau \cos \zeta$, where ζ is the root of

$$\zeta = \begin{cases} -a\tau \tan \zeta, & 0 < \zeta < \pi, & a \neq 0, \\ \pi/2, & & a = 0. \end{cases}$$

Theorem 5.2. (1) If (20) is satisfied, then the trivial steady state \mathbf{S}_0 is locally asymptotically stable.
 (2) If (20) is not satisfied, then the trivial steady state \mathbf{S}_0 is unstable.

Proof. We linearize the system (8) around \mathbf{S}_0 . Then, we obtain

$$\begin{cases} \frac{d}{dt}x(t) &= -\mu_w x(t) + e^{-\mu\tau} P_w x(t - \tau), \\ \frac{d}{dt}y(t) &= -\mu_u y(t) + e^{-\mu\tau} P_{wu} x(t - \tau) + e^{-\mu\tau} P_u y(t - \tau). \end{cases}$$

The corresponding characteristic equation is given by

$$\det(\lambda I - A - Be^{-\lambda\tau}) = 0,$$

with

$$A = \begin{pmatrix} -\mu_w & 0 \\ 0 & -\mu_u \end{pmatrix} \quad \text{and} \quad B = e^{-\mu\tau} \begin{pmatrix} P_w & 0 \\ P_{wu} & P_u \end{pmatrix}$$

and I the 2×2 identity matrix. Therefore,

$$(\lambda + \mu_w - P_w e^{-\mu\tau} e^{-\lambda\tau})(\lambda + \mu_u - P_u e^{-\mu\tau} e^{-\lambda\tau}) = 0. \quad (21)$$

The objective is to find conditions such that the solutions of (21) have negative real parts. We have to analyze separately the solutions of each factor of the product given by (21). For the equation

$$\lambda + \mu_j - P_j e^{-\mu\tau} e^{-\lambda\tau} = 0, \quad j \in \{u, w\},$$

the statement (i) $a\tau = \mu_j\tau > -1$ of Lemma 5.1, is always satisfied. On the other hand, the condition (ii) $a + b = \mu_j - P_j e^{-\mu\tau} > 0$ of Lemma 5.1, is equivalent to

$$\tau > \tau_j := \frac{1}{\mu} \ln(\delta_j), \quad j \in \{u, w\}.$$

For the statement (iii) of Lemma 5.1, as $a \neq 0$, we remark that the condition $0 < \zeta < \pi$, implies that $\sin \zeta > 0$. Then, the relation $\zeta = -\mu_j\tau \tan \zeta$ means that $\cos \zeta < 0$. Thus, $\pi/2 < \zeta < \pi$. Consequently, the statement (iii) is always satisfied for $\tau > 0$. We conclude that the conditions (i)-(iii) of Lemma 5.1, can be summed up in

$$\tau > \max\{0, \tau_u, \tau_w\}.$$

This concludes the proof of Theorem 5.2. \square

12

5.2. Global asymptotic stability of the trivial steady state \mathbf{S}_0

Let's write the nonlinear system (8) in the following general form

$$\begin{cases} \frac{dx}{dt} = Ax(t) + F(x(t-\tau)), & t > 0, \\ x(t) = \phi(t), & t \in [-\tau, 0], \end{cases} \quad (22)$$

where

$$A = \begin{bmatrix} -\mu_w & 0 \\ 0 & -\mu_u \end{bmatrix}, \quad x(t) = \begin{bmatrix} w(t) \\ u(t) \end{bmatrix}, \quad F(y) = \begin{bmatrix} f_1(y_1, y_2) \\ f_2(y_1, y_2) \end{bmatrix},$$

with

$$\begin{cases} f_1(y_1, y_2) = P_w e^{-\mu\tau} y_1 e^{-(y_1+y_2)^\eta}, \\ f_2(y_1, y_2) = (P_u y_2 + P_{wu} y_1) e^{-\mu\tau} e^{-(y_1+y_2)^\eta}. \end{cases}$$

To prove our result (Theorem 5.4) on the global asymptotic stability of the trivial steady state, we use the following lemma.

Lemma 5.3. ([6, 25]). *Suppose that there exists $\gamma > 0$ such that, for all $y \in \mathbb{R}_+^2$,*

$$\|F(y)\| \leq \gamma \|y\| \quad \text{and} \quad \gamma < -\theta(A),$$

where $\|\cdot\|$ is a norm in \mathbb{R}^2 and $\theta(A)$ is the matrix measure of A ,

$$\theta(A) = \lim_{\epsilon \rightarrow 0^+} \frac{\|I + \epsilon A\| - 1}{\epsilon}.$$

Then, the trivial equilibrium of (22) is globally asymptotically stable.

Theorem 5.4. *Suppose that*

$$\tau > \frac{1}{\mu} \ln \left(\frac{\max\{P_w, P_u + P_{wu}\}}{\min\{\mu_w, \mu_u\}} \right).$$

Then, the trivial steady state \mathbf{S}_0 of the system (8) is globally asymptotically stable.

Proof. We have to find $0 < \gamma < -\theta(A)$, such that $\|F(y)\| \leq \gamma \|y\|$, for all $y \in \mathbb{R}_+^2$. We choose the norm $\|x\| = \max\{|w|, |u|\}$ in \mathbb{R}^2 . Then,

$$\|F(y)\| \leq e^{-\mu\tau} \max\{P_w, P_u + P_{wu}\} \|y\| := \gamma \|y\|.$$

We also have

$$\begin{aligned} \theta(A) &= \lim_{\epsilon \rightarrow 0^+} \frac{\|I + \epsilon A\| - 1}{\epsilon}, \\ &= \lim_{\epsilon \rightarrow 0^+} \frac{\max\{1 - \epsilon\mu_w, 1 - \epsilon\mu_u\} - 1}{\epsilon}, \\ &= \lim_{\epsilon \rightarrow 0^+} \frac{1 - \epsilon \min\{\mu_w, \mu_u\} - 1}{\epsilon}, \\ &= -\min\{\mu_w, \mu_u\}. \end{aligned}$$

Finally, provided that

$$0 < e^{-\mu\tau} \max\{P_w, P_u + P_{wu}\} < \min\{\mu_w, \mu_u\}, \quad (23)$$

Lemma 5.3 guarantees the global asymptotic stability of the trivial steady state \mathbf{S}_0 . In fact, the condition (23) is equivalent to

$$\tau > \frac{1}{\mu} \ln \left(\frac{\max\{P_w, P_u + P_{wu}\}}{\min\{\mu_w, \mu_u\}} \right).$$

This finishes the proof of the theorem. \square

Remark 5.5. It is not difficult to see that the condition

$$\tau > \frac{1}{\mu} \ln \left(\frac{\max\{P_w, P_u + P_{wu}\}}{\min\{\mu_w, \mu_u\}} \right)$$

implies in particular that

$$\tau > \max\{0, \tau_u, \tau_w\}.$$

The local asymptotic stability of the other steady states will be analyzed by increasing the delay τ from zero with the possibility of eigenvalues to cross on the imaginary axis and the appearance of Hopf bifurcation.

5.3. Local asymptotic stability and Hopf bifurcation of *Wolbachia*-free steady state \mathbf{S}_u

The *Wolbachia*-free steady state $\mathbf{S}_u := (0, (\ln R_u)^{\frac{1}{\eta}})$, $R_u = \delta_u e^{-\mu\tau}$, exists only in the scenarios (ii)-(a) and (iv)-(a) of Proposition 4.3. That is under the condition

$$0 \leq \tau < \tau_u.$$

The linearization of the system (8) around the steady state \mathbf{S}_u is given by

$$\begin{cases} \frac{d}{dt}x(t) &= -\mu_w x(t) + \frac{P_w}{\delta_u} x(t - \tau), \\ \frac{d}{dt}y(t) &= -\mu_u y(t) + \frac{P_{wu}}{\delta_u} x(t - \tau) + \frac{P_u}{\delta_u} (1 - \eta \ln(R_u)) y(t - \tau). \end{cases} \quad (24)$$

Note that $P_u = \mu_u \delta_u$, $P_w = \mu_w \delta_w$ and $P_{wu} = \mu_u \delta_{wu}$. Then, the characteristic equation associate to (24) is given by

$$\left(\lambda + \mu_w - \mu_w \frac{\delta_w}{\delta_u} e^{-\lambda\tau} \right) (\lambda + \mu_u - \mu_u (1 - \eta \ln(R_u)) e^{-\lambda\tau}) = 0. \quad (25)$$

The roots of the first term of the characteristic equation (see Lemma 5.1),

$$\lambda + \mu_w - \mu_w \frac{\delta_w}{\delta_u} e^{-\lambda\tau} = 0,$$

have negative real parts if and only if

- (i) $\mu_w \tau > -1$,
- (ii) $\tilde{\delta}_u > \delta_w$,
- (iii) $-\tau \mu_w \frac{\delta_w}{\delta_u} < \zeta \sin \zeta - \mu_w \tau \cos \zeta$, where ζ is the root of

$$\zeta = -\mu_w \tau \tan \zeta, \quad 0 < \zeta < \pi.$$

The statements (i) and (iii) are always satisfied and the statement (ii) is equivalent to

$$\tau_u > \tau_w.$$

Then, we can immediately conclude the following result.

14

Proposition 5.6. *Suppose that*

$$\tau_u \leq \tau_w \quad \text{and} \quad 0 \leq \tau < \tau_u.$$

Then, the steady state \mathbf{S}_u is unstable.

Now suppose that

$$\tau_u > \tau_w.$$

Then, the local asymptotic stability of the steady state \mathbf{S}_u is given by the roots of the second term of the characteristic equation (25):

$$\lambda + \mu_u - \mu_u (1 - \eta \ln(R_u)) e^{-\lambda\tau} = 0. \quad (26)$$

Thanks to Lemma 5.1, the roots of (26) have negative real parts if and only if

- (i) $\mu_u \tau > -1$,
- (ii) $R_u > 1$,
- (iii) $-\tau \mu_u (1 - \eta \ln(R_u)) < \zeta \sin \zeta - \tau \mu_u \cos \zeta$, where ζ is the root of

$$\zeta = -\tau \mu_u \tan \zeta, \quad 0 < \zeta < \pi.$$

The statement (i) is always satisfied and the statement (ii) is equivalent to the condition that gives the existence of the steady state \mathbf{S}_u . Suppose that

$$\eta > \frac{1}{\ln(R_u)}. \quad (27)$$

Then, the statement (iii) is satisfied and we have the local asymptotic stability of the steady state \mathbf{S}_u . In fact, the condition (27) is equivalent to

$$\max \left\{ 0, \tau_u - \frac{1}{\eta \mu} \right\} < \tau < \tau_u. \quad (28)$$

We directly conclude the following result.

Proposition 5.7. *If the condition (28) is satisfied then, the steady state \mathbf{S}_u is locally asymptotically stable. In particular, if*

$$\eta < \frac{1}{\ln(\delta_u)},$$

then, for all $0 \leq \tau < \tau_u$, \mathbf{S}_u is locally asymptotically stable.

Now suppose that

$$\eta > \frac{1}{\ln(\delta_u)}.$$

This inequality is equivalent to

$$\bar{\tau}_u := \tau_u - \frac{1}{\eta \mu} > 0.$$

We proved that \mathbf{S}_u is locally asymptotically stable for $\bar{\tau}_u < \tau < \tau_u$. Suppose that

$$0 \leq \tau < \bar{\tau}_u.$$

When $\tau = 0$, the characteristic equation (26) reads

$$\Delta(0, \lambda) = \lambda + \mu_u - \mu_u (1 - \eta \ln(\delta_u)) = 0.$$

It has only one root

$$\lambda_0 = -\mu_u \eta \ln(\delta_u) \in \mathbb{R}.$$

As $\delta_u > 1$, then $\lambda_0 < 0$. We conclude that the steady state \mathbf{S}_u is locally asymptotically stable for $\tau = 0$. By using a continuity argument, it is straightforward that there exists $\varrho \in (0, \bar{\tau}_u)$, such that \mathbf{S}_u is locally

asymptotically stable for $\tau \in [0, \varrho)$. Consequently, when $\tau \in [0, \tilde{\tau}_u)$ increases, the stability of \mathbf{S}_u can only be lost if characteristic roots cross on the imaginary axis. We look for purely imaginary roots $\pm i\omega$, $\omega \in \mathbb{R}$. Remark that if λ is a characteristic root then its conjugate $\bar{\lambda}$ is also a characteristic root. Then, we look for purely imaginary roots $i\omega$ with $\omega > 0$. By separating real and imaginary parts in the characteristic equation (26), we get

$$\begin{cases} \mu_u(1 - \eta \ln(R_u)) \cos(\tau\omega) &= \mu_u, \\ \mu_u(1 - \eta \ln(R_u)) \sin(\tau\omega) &= -\omega. \end{cases} \quad (29)$$

Adding the squares of both hand sides of the last system and using the fact that $\cos^2(\tau\omega) + \sin^2(\tau\omega) = 1$, it follows that

$$\frac{\omega^2}{\mu_u^2} = \eta \ln(R_u) (\eta \ln(R_u) - 2).$$

For the existence of $\omega > 0$, it is necessary to have

$$0 < \tau < \tilde{\tau}_u := \tau_u - \frac{2}{\eta\mu}.$$

Then, it is immediate to conclude the following result.

Proposition 5.8. *If*

$$\eta < \frac{2}{\ln(\delta_u)}$$

then, for all $0 \leq \tau < \tau_u$, \mathbf{S}_u is locally asymptotically stable.

Now suppose that

$$\eta > \frac{2}{\ln(\delta_u)}$$

and consider the function $\varpi: [0, \tilde{\tau}_u) \rightarrow (0, +\infty)$ defined by

$$\varpi(\tau) = \mu_u \sqrt{\eta \ln(R_u) (\eta \ln(R_u) - 2)}, \quad \text{for all } \tau \in [0, \tilde{\tau}_u).$$

In fact, we have

$$\varpi(\tau) = \eta\mu\mu_u \sqrt{(\tau_u - \tau)(\tilde{\tau}_u - \tau)}, \quad \text{for all } \tau \in [0, \tilde{\tau}_u). \quad (30)$$

Then, for each $\tau \in [0, \tilde{\tau}_u)$, there is a unique solution $\Theta(\tau) \in [0, 2\pi)$ of the system

$$\begin{cases} \cos(\Theta(\tau)) &= -\frac{1}{\eta\mu(\tilde{\tau}_u - \tau) + 1} < 0, \\ \sin(\Theta(\tau)) &= \frac{\eta\mu\sqrt{(\tau_u - \tau)(\tilde{\tau}_u - \tau)}}{\eta\mu(\tilde{\tau}_u - \tau) + 1} > 0. \end{cases}$$

Then, $\Theta(\tau) \in (\pi/2, \pi)$ and it is given by

$$\Theta(\tau) = \arccos\left(-\frac{1}{\eta\mu(\tilde{\tau}_u - \tau) + 1}\right). \quad (31)$$

We conclude that the system (29) is equivalent to find $\tau \in [0, \tilde{\tau}_u)$ solution of

$$\tau\varpi(\tau) = \Theta(\tau) + 2k\pi, \quad k \in \mathbb{N},$$

with $\varpi(\tau)$ given by (30) and $\Theta(\tau)$ by (31). We remark here that in all this study, the set \mathbb{N} includes 0. This is equivalent to solve

$$Z_k(\tau) := \tau - \frac{1}{\varpi(\tau)} [\Theta(\tau) + 2k\pi] = 0, \quad k \in \mathbb{N}, \quad \tau \in [0, \tilde{\tau}_u).$$

16

More precisely, we have to solve for $k \in \mathbb{N}$ and $\tau \in [0, \tilde{\tau}_u)$,

$$Z_k(\tau) := \tau - \frac{1}{\eta\mu\mu_u\sqrt{(\tau_u - \tau)(\tilde{\tau}_u - \tau)}} \left[\arccos\left(-\frac{1}{\eta\mu(\tilde{\tau}_u - \tau) + 1}\right) + 2k\pi \right] = 0. \quad (32)$$

The functions $Z_k(\tau)$ are given explicitly. However, we cannot determine explicitly their roots. The roots can be found numerically. The following lemma states some properties of the functions Z_k , $k \in \mathbb{N}$.

Lemma 5.9. *For all $k \in \mathbb{N}$ and $\tau \in [0, \tilde{\tau}_u)$,*

$$Z_k(0) < 0, \quad Z_{k+1}(\tau) < Z_k(\tau) \quad \text{and} \quad \lim_{\tau \rightarrow \tilde{\tau}_u} Z_k(\tau) = -\infty.$$

Therefore, provided that no root of Z_k is a local extremum, the number of positive roots of Z_k , $k \in \mathbb{N}$, on the interval $[0, \tilde{\tau}_u)$ is even.

This lemma implies, in particular, that, if Z_k has no root on $[0, \tilde{\tau}_u)$, then no function Z_j , with $j > k$, has roots on $[0, \tilde{\tau}_u)$. The next proposition is a direct consequence of Lemma 5.9.

Proposition 5.10. *If the function Z_0 defined on the interval $[0, \tilde{\tau}_u)$, by*

$$Z_0(\tau) := \tau - \frac{\arccos\left(-\frac{1}{\eta\mu(\tilde{\tau}_u - \tau) + 1}\right)}{\eta\mu\mu_u\sqrt{(\tau_u - \tau)(\tilde{\tau}_u - \tau)}} \quad (33)$$

has no root, then the steady state \mathbf{S}_u is locally asymptotically stable for all $\tau \in [0, \tilde{\tau}_u)$.

We now suppose that Z_0 , under the condition

$$\eta > \frac{2}{\ln(\delta_u)},$$

has at least one positive root on the interval $[0, \tilde{\tau}_u)$. Let $\tau_u^* \in (0, \tilde{\tau}_u)$ be the smallest root of Z_0 . Then, \mathbf{S}_u is locally asymptotically stable for $\tau \in [0, \tau_u^*)$, and loses its stability when $\tau = \tau_u^*$. A finite number of stability switch may occurs as τ increases and passes through roots of the Z_k functions.

Our next objective is to prove that \mathbf{S}_u can be destabilized through a Hopf bifurcation as $\tau \in [0, \tilde{\tau}_u)$ increases. We start by proving that if an imaginary characteristic root $i\omega$ exists then, it is simple. Suppose, by contradiction, that $\lambda = i\omega$ is not a simple characteristic root. Then, λ is a solution of

$$\Delta(\tau, \lambda) = 0 \quad \text{and} \quad \frac{\partial}{\partial \lambda} \Delta(\tau, \lambda) = 0,$$

where

$$\Delta(\tau, \lambda) = \lambda + \mu_u - \mu_u (1 - \eta \ln(R_u)) e^{-\lambda\tau}. \quad (34)$$

This is equivalent to

$$\begin{cases} e^{\lambda\tau} [\lambda + \mu_u] &= \mu_u [1 - \eta \ln(R_u)], \\ e^{\lambda\tau} &= -\tau\mu_u [1 - \eta \ln(R_u)]. \end{cases} \quad (35)$$

The two equations of the system (35) lead to

$$(\lambda + \mu_u)\tau + 1 = 0.$$

This a contradiction with the fact that $\lambda = i\omega$.

As τ_u^* is the smallest root of Z_0 then, from the definition of Z_0 , the characteristic equation (34) has purely imaginary roots $\pm i\varpi(\tau_u^*)$, where ϖ is defined by (30). The stability of the positive steady state switches from stable to unstable as τ passes through τ_u^* . Other stability switch occur when τ passes through roots of the Z_k functions (see [4]).

Now, we rewrite the characteristic equation (34) in the following form

$$\Delta(\tau, \lambda) := A(\tau, \lambda) + B(\tau)e^{-\lambda\tau} = 0.$$

We define, for $\lambda = i\omega$, the polynomial function

$$H(\tau, \omega) := |A(\tau, i\omega)|^2 - |B(\tau)|^2.$$

Then,

$$H(\tau, \omega) = \omega^2 - \eta^2 \mu^2 \mu_u^2 (\tau_u - \tau) (\tilde{\tau}_u - \tau).$$

Let $\lambda(\tau)$ be a branch of roots of (34) such that $\lambda(\tau_u^*) = i\varpi(\tau_u^*)$. The Hopf bifurcation theorem says that a Hopf bifurcation occurs at \mathbf{S}_u when $\tau = \tau_u^*$ if

$$\text{sign} \left[\left(\frac{d\Re(\lambda(\tau))}{d\tau} \right)_{\tau=\tau_u^*} \right] > 0.$$

We know from [4] that

$$\text{sign} \left[\left(\frac{d\Re(\lambda(\tau))}{d\tau} \right)_{\tau=\tau_u^*} \right] = \text{sign} \left(\frac{\partial h}{\partial z}(\tau_u^*, \varpi^2(\tau_u^*)) \right) \text{sign} \left(\frac{dZ_0(\tau_u^*)}{d\tau} \right),$$

with

$$h(\tau, \omega^2) := H(\tau, \omega).$$

That is to say

$$h(\tau, z) = z - \eta^2 \mu^2 \mu_u^2 (\tau_u - \tau) (\tilde{\tau}_u - \tau).$$

It is clear that

$$\frac{\partial h}{\partial z}(\tau_u^*, \varpi^2(\tau_u^*)) = 1.$$

It follows

$$\text{sign} \left[\left(\frac{d\Re(\lambda(\tau))}{d\tau} \right)_{\tau=\tau_u^*} \right] = \text{sign} \left(\frac{dZ_0(\tau_u^*)}{d\tau} \right).$$

The following proposition states the existence of a Hopf bifurcation at $\tau = \tau_u^*$ that destabilizes the positive steady state \mathbf{S}_u .

Proposition 5.11. *If $Z_0(\tau)$ has at least one positive root on the interval $(0, \tilde{\tau}_u)$, then the positive steady state \mathbf{S}_u is locally asymptotically stable for $\tau \in [0, \tau_u^*)$, where τ_u^* is the smallest root of $Z_0(\tau)$ on $(0, \tilde{\tau}_u)$, and \mathbf{S}_u loses its stability when $\tau = \tau_u^*$. A finite number of stability switch may occur as τ passes through roots of the Z_k functions. Moreover, if*

$$\frac{dZ_0(\tau_u^*)}{d\tau} > 0,$$

then a Hopf bifurcation occurs at \mathbf{S}_u for $\tau = \tau_u^$.*

Figure 2 shows, for two set of parameters, the existence or non-existence of roots for the functions Z_0 and Z_1 , given by the equation (32). In each case, $\tau \in (0, \tilde{\tau}_u)$. On the left, we have $\eta = 2.0$ and no root for Z_k . Then, the equilibrium \mathbf{S}_u stays locally asymptotically stable on the interval $(0, \tilde{\tau}_u)$. On the right, we have $\eta = 3.0$ and two roots for Z_0 (no root for Z_1). A Hopf bifurcation occurs at $\tau = \tau_u^*$ and periodic oscillations around the

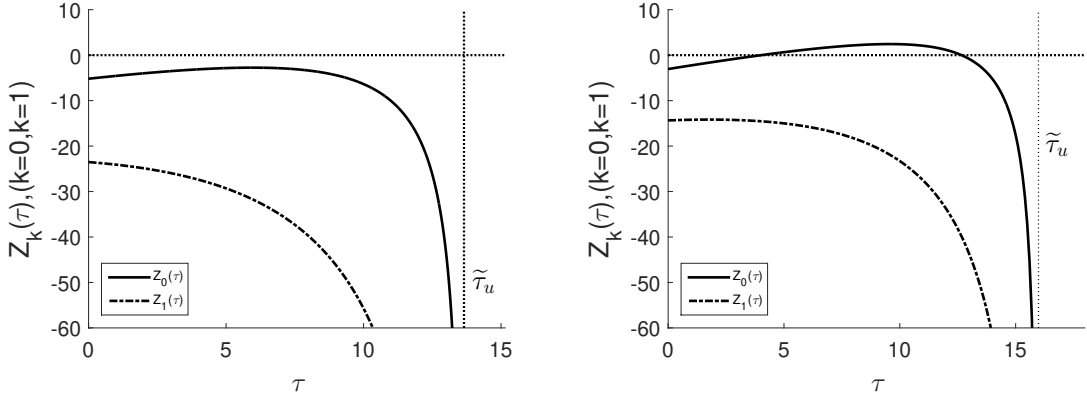


FIGURE 2. The functions Z_k , $k = 0, 1$, given by the equation (32), versus τ . On the left, we can see that Z_0 and Z_1 have no roots. The vertical line shows the right end of Z_k domain, $\tilde{\tau}_u = 13.65$. On the right, we can see that Z_0 has two roots $\tau_u^* = 4.01$ and $\tau_u^+ = 12.67$, and Z_1 has no root. The vertical line shows the right end of Z_k domain $\tilde{\tau}_u = 15.98$. At $\tau = \tau_u^*$ a Hopf bifurcation occurs and periodic oscillations around the equilibrium are observed until $\tau = \tau_u^+$; outside the interval (τ_u^*, τ_u^+) , the equilibrium \mathbf{S}_u is locally asymptotically stable. In both panels, we use the parameter set from case (ii) (Table 1). On the left, we set $\eta = 2.0$, and on the right, we set $\eta = 3.0$.

equilibrium \mathbf{S}_u are observed until the threshold $\tau = \tau_u^+$. The equilibrium \mathbf{S}_u corresponds to the extinction of *Wolbachia*-infected mosquito and the persistence of uninfected one.

For the set of parameters given in the case (ii), Table 1, where the equilibrium \mathbf{S}_u exists for $\tau \in [0, \tau_u)$, we can see in Figure 3, for each value of η , the roots of Z_0 . For η less than a threshold, η_{\min} ($\eta_{\min} \approx 2$), Z_0 has no root which implies that the steady state \mathbf{S}_u is stable. For η greater than η_{\min} , Z_0 has two roots τ_u^* and τ_u^+ . In this case, \mathbf{S}_u loses stability at $\tau = \tau_u^*$ and periodic oscillations can be seen. For $\tau = \tau_u^+$ the stability of \mathbf{S}_u is recovered. The equilibrium \mathbf{S}_u corresponds to the extinction of *Wolbachia*-infected mosquito and persistence of uninfected one.

Using the set of parameters from case (ii), Table 1, and $\eta = 3.0$, in Figure 4, we can see in the panel (a) the minimum and the maximum values of the periodic solutions $u(t)$ of the system (8) plotted for $\tau_u^* \leq \tau < \tau_u^+$ (where \mathbf{S}_u is unstable). This corresponds to the amplitude of $u(t)$ for $\tau_u^* \leq \tau < \tau_u^+$. In the panel (b), we plotted the period of these periodic oscillations which is an increasing function of $\tau \in (\tau_u^*, \tau_u^+)$. Finally in the panel (c), we can see an example of temporal evolution of the system (8) for $\eta = 3.0$ and $\tau = 10$. The component $u(t)$ oscillates around the steady state and the component $w(t)$ tends to zero with positive damped oscillations.

5.4. Local asymptotic stability of the coexistence steady state \mathbf{S}_{wu}

The coexistence steady state

$$\mathbf{S}_{wu} = (w^*, u^*) := \left((\ln R_w)^{\frac{1}{\eta}} (1 - \beta_{wu}), (\ln R_w)^{\frac{1}{\eta}} \beta_{wu} \right),$$

with $R_w = \delta_w e^{-\mu\tau}$ and $\beta_{wu} = \frac{\delta_{wu}}{\delta_w - \delta_u + \delta_{wu}}$, exists only under the condition

$$\tau_u < \tau_w \quad \text{and} \quad 0 \leq \tau < \tau_w.$$

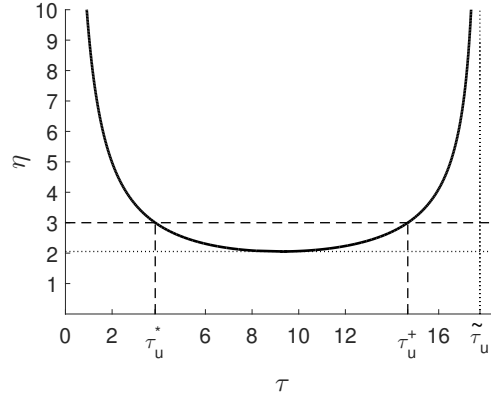


FIGURE 3. η versus τ . The continuous curve provides the roots of $Z_0(\tau)$ given η (see 33). For the set of parameters chosen, case (ii) (Table 1), the horizontal dotted line highlights the lower threshold to have Hopf bifurcation. The domain of Z_0 is given by $(0, \tilde{\tau}_u)$ with $\tilde{\tau}_u = 17.76$. As an example, the dashed line is set for $\eta = 3.0$. For this value of η , the corresponding roots of Z_0 are $\tau_u^* = 3.85$ and $\tau_u^+ = 14.67$. As $dZ_0(\tau_u^*)/d\tau > 0$ a Hopf bifurcation occurs at $\tau = \tau_u^*$ by Proposition 5.11. At this point, the equilibrium \mathbf{S}_u loses his stability and periodic oscillations can be seen until τ_u^+ . At $\tau = \tau_u^+$ the stability of \mathbf{S}_u is recovered. This corresponds to the extinction of *Wolbachia*-infected mosquito and persistence of uninfected one.

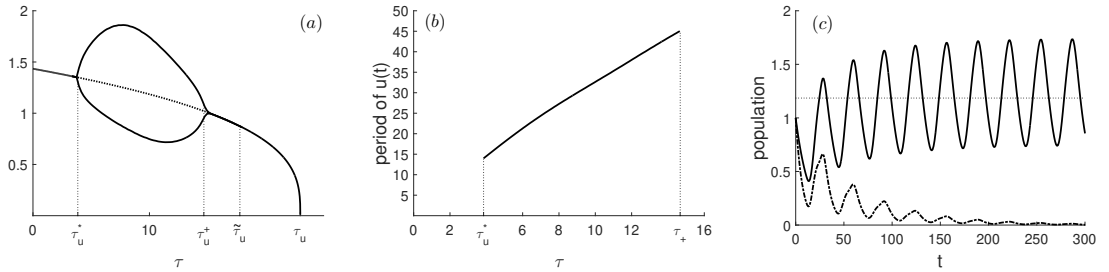


FIGURE 4. From the left to the right we have: (a) the minimum and the maximum values of the component $u(t)$ of the system (8) plotted against $\tau \in (\tau_u^*, \tau_u^+)$; (b) the period of the oscillations of $u(t)$ versus $\tau \in (\tau_u^*, \tau_u^+)$; and (c) the temporal evolution of $u(t)$ (solid line) and $w(t)$ (dot-dash line) given by the system (8) with $\tau = 10$. In all panels, the parameters were taken from Table 1 case (iv) and $\eta = 3$. The thresholds given by $\tau_u^* = 3.85$, $\tau_u^+ = 14.67$, $\tilde{\tau}_u = 17.76$ and $\tau_u = 22.95$ are, respectively, the first and second roots of Z_0 , the right end of the domain of the function Z_0 , and the right end of τ that allows the existence of \mathbf{S}_u .

The linearization of the system (8) around the steady state \mathbf{S}_{wu} is given by

$$\begin{cases} \frac{d}{dt}x(t) &= -\mu_w x(t) + b_{11}x(t-\tau) + b_{12}y(t-\tau), \\ \frac{d}{dt}y(t) &= -\mu_u y(t) + b_{21}x(t-\tau) + b_{22}y(t-\tau), \end{cases}$$

20

with

$$\begin{cases} b_{11} &= P_w e^{-\mu\tau} e^{-(w^*+u^*)^\eta} (1 - \eta w^* (w^* + u^*)^{\eta-1}), \\ b_{12} &= -\eta P_w e^{-\mu\tau} e^{-(w^*+u^*)^\eta} w^* (w^* + u^*)^{\eta-1}, \\ b_{21} &= e^{-\mu\tau} e^{-(w^*+u^*)^\eta} (P_{wu} - \eta(P_u u^* + P_{wu} w^*) (w^* + u^*)^{\eta-1}), \\ b_{22} &= e^{-\mu\tau} e^{-(w^*+u^*)^\eta} (P_u - \eta(P_u u^* + P_{wu} w^*) (w^* + u^*)^{\eta-1}). \end{cases}$$

When $\tau = 0$, the Jacobian matrix evaluated at $\mathbf{S}_{\mathbf{w}\mathbf{u}}$ is given by

$$\mathbf{J}(\mathbf{S}_{\mathbf{w}\mathbf{u}}) = \begin{bmatrix} -\eta\mu_w(1 - \beta_{wu}) \ln(\delta_w) & -\eta\mu_w(1 - \beta_{wu}) \ln(\delta_w) \\ \frac{P_{wu}}{\delta_w} - \eta\mu_u\beta_{wu} \ln(\delta_w) & \frac{P_u}{\delta_w} - \eta\mu_u\beta_{wu} \ln(\delta_w) - \mu_u \end{bmatrix}.$$

Hence, the eigenvalues λ of $J(\mathbf{S}_{\mathbf{w}\mathbf{u}})$ satisfy the characteristic equation

$$\begin{aligned} \lambda^2 + \lambda \left(-\frac{P_u}{\delta_w} + \eta\mu_w(1 - \beta_{wu}) \ln(\delta_w) + \eta\mu_u\beta_{wu} \ln(\delta_w) + \mu_u \right) \\ + \left(\frac{P_{wu} - P_u}{\delta_w} + \mu_u \right) \eta\mu_w(1 - \beta_{wu}) \ln(\delta_w) = 0. \end{aligned}$$

Thus, by the Routh-Hurwitz criterion, the steady state $\mathbf{S}_{\mathbf{w}\mathbf{u}}$ is stable when the following conditions are satisfied.

$$\begin{cases} \mu_u \left(1 - \frac{\delta_u}{\delta_w} \right) + \eta\mu_w(1 - \beta_{wu}) \ln(\delta_w) + \eta\mu_u\beta_{wu} \ln(\delta_w) &> 0, \\ \eta\mu_u\mu_w \left(\frac{\delta_{wu} + \delta_w - \delta_u}{\delta_w} \right) (1 - \beta_{wu}) \ln(\delta_w) &> 0. \end{cases}$$

Remember that the condition for the existence of $\mathbf{S}_{\mathbf{w}\mathbf{u}}$ for $\tau = 0$, is given by

$$\delta_u < \delta_w \quad \text{and} \quad \delta_w > 1.$$

This means in particular, that $0 < \beta_{wu} < 1$. We conclude that the steady state $\mathbf{S}_{\mathbf{w}\mathbf{u}}$ is always locally asymptotically stable for $\tau = 0$. Thus, it is straightforward that there exists $\varrho \in (0, \tau_w)$, such that $\mathbf{S}_{\mathbf{w}\mathbf{u}}$ is locally asymptotically stable for $\tau \in [0, \varrho)$. Consequently, when $\tau \in [0, \tau_w)$ increases, the stability of $\mathbf{S}_{\mathbf{w}\mathbf{u}}$ can only be lost if characteristic roots cross on the imaginary axis. Indeed, we showed numerically that this really happens and, similarly to $\mathbf{S}_{\mathbf{u}}$, there exists Hopf bifurcation for $\mathbf{S}_{\mathbf{w}\mathbf{u}}$. As an example, we plotted Figure 5. In (a), we can see for each value of $\eta > 0$ the corresponding values of τ that limit the region where the equilibrium $\mathbf{S}_{\mathbf{w}\mathbf{u}}$ is stable and unstable (with periodic oscillations). For $\eta = 4$, a Hopf bifurcation occurs at $\tau \approx 3.5$ and the stability of $\mathbf{S}_{\mathbf{w}\mathbf{u}}$ is restored at $\tau \approx 8.2$. For values of $\tau \in [3.5, 8.2[$ the temporal behaviour of the system (8) shows periodic oscillations around $\mathbf{S}_{\mathbf{w}\mathbf{u}}$.

6. DISCUSSION

Starting from an age structured partial differential model (4-equations), constructed taking into account the mosquito life cycle and the main features of the *Wolbachia*-infection, we derived a delay differential model (2-equations) using the method of characteristics, to study the colonization and persistence of the *Wolbachia*-transinfected *Aedes aegypti* mosquito in an environment where the uninfected wild mosquito population is already established. The reduction of the model to a delay differential system permits that several important and interesting questions, such as the equilibriums and their local and global stability, can be analytically addressed while keeping all the biological assumptions behind the model.

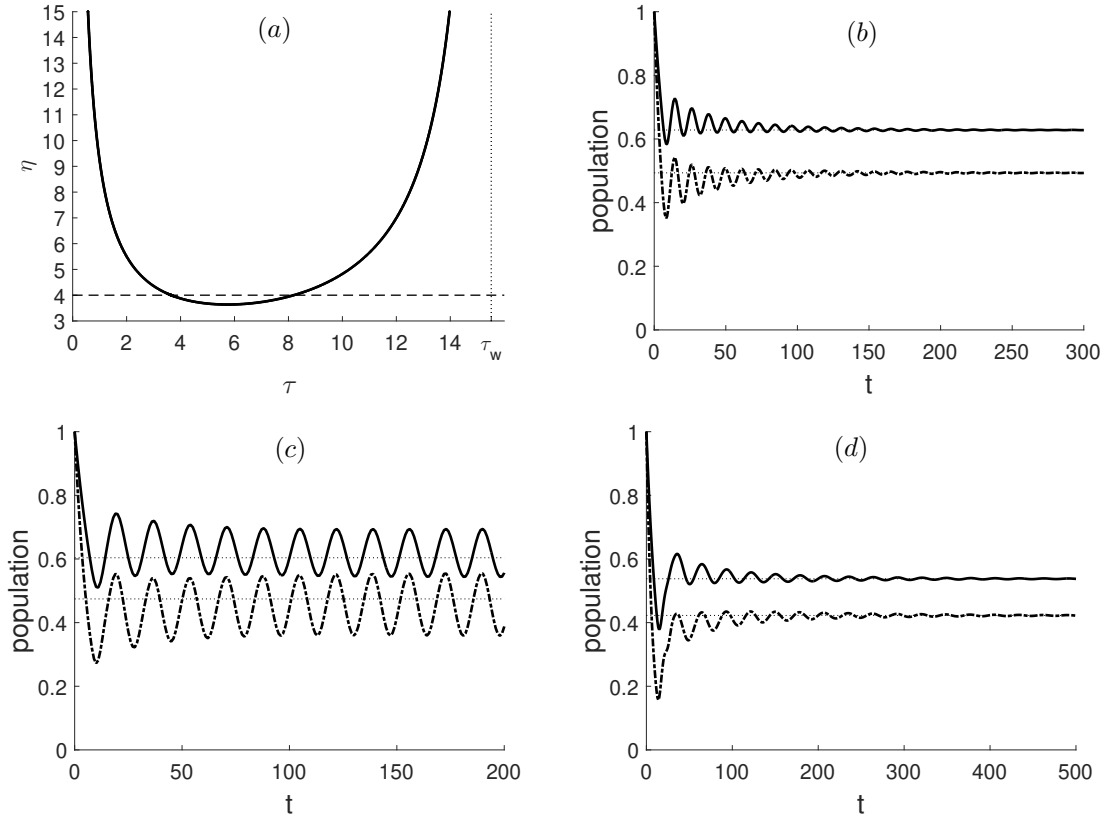


FIGURE 5. In (a), η versus τ (it was obtained using the package DDE-BIFTOOL v. 3.1.1 and MATLAB R2019). For $\eta = 4$ the panels (b), (c) and (d) show the temporal evolution of $u(t)$ (solid line) and $w(t)$ (dot-dash line) given by (8) with $\tau = 3.2$, $\tau = 5$ and $\tau = 8.9$, respectively. The other parameters were taken from the case (iv) of Table 1. A Hopf bifurcation occurs at $\tau \approx 3.5$ and the stability of $\mathbf{S}_{\mathbf{w}\mathbf{u}}$ is restored at $\tau \approx 8.2$; $\tau \in (0, 22.33)$.

Thus, the positivity, boundedness and uniqueness of solutions were proved. The model admits three steady states: extinction of both populations (\mathbf{S}_0), extinction of infected population and persistence of uninfected population (\mathbf{S}_u), and persistence of both populations ($\mathbf{S}_{\mathbf{w}\mathbf{u}}$). The conditions of existence of each equilibrium were established as a combination of the entomological parameters that describe mosquito life's cycle (such as mortality, oviposition and development rates) and the effects of the *Wolbachia* presence in the host (vertical transmission of the bacteria, cytoplasmic incompatibility, and sex-ratio-distorting). The two thresholds R_w and R_u can be interpreted as the net reproductive rates which are defined as the average numbers of female offspring that a female produces during her lifetime. Therefore, R_w measured the number of infected offspring produced by an infected female and R_u measured the number of uninfected offspring produced by an uninfected female. Moreover, we could prove that \mathbf{S}_0 always exists, \mathbf{S}_u exists if and only if $R_u > 1$ and $\mathbf{S}_{\mathbf{w}\mathbf{u}}$ exists if and only if $R_w > \max\{1, R_u\}$.

As we were interested in analyzing the effect of variation on developmental time in population dynamics, we rewrote the condition of existence of each equilibrium in terms of the delay τ which measures the time spent

from egg to adult. Four scenarios can be drawn (Figure 1): (i) assume that $\tau_u, \tau_w \leq 0$ (these thresholds are equivalent to the ones on R_u and R_w , respectively). Then, for all $\tau \geq 0$, \mathbf{S}_0 is the only steady state; (ii) assume that $\tau_u > 0$ and $\tau_w \leq \tau_u$. Then, if $0 \leq \tau < \tau_u$, there are two steady states \mathbf{S}_0 and \mathbf{S}_u , and if $\tau \geq \tau_u$, \mathbf{S}_0 is the only steady state; assume that $\tau_u \leq 0 < \tau_w$. Then, if $0 \leq \tau < \tau_w$, there are two steady states \mathbf{S}_0 and \mathbf{S}_{wu} , if $\tau \geq \tau_w$, \mathbf{S}_0 is the only steady state; (iv) assume that $0 < \tau_u < \tau_w$. Then, if $0 \leq \tau < \tau_u$, there are three steady states \mathbf{S}_0 , \mathbf{S}_u and \mathbf{S}_{wu} , if $\tau_u \leq \tau < \tau_w$, there are two steady states \mathbf{S}_0 and \mathbf{S}_{wu} , and if $\tau \geq \tau_w$, \mathbf{S}_0 is the only steady state.

The global stability of \mathbf{S}_0 was obtained under the condition $\tau > \frac{1}{\mu} \ln(\max\{P_w, P_u + P_{wu}\} / \min\{\mu_w, \mu_u\})$. Therefore, the increase of the immature development time τ (which could occur under decreasing temperature for example) leads both populations to extinction. Interestingly, the increase of the delay can also destabilize, by a Hopf bifurcation, the equilibriums \mathbf{S}_u and \mathbf{S}_{wu} . For the equilibrium \mathbf{S}_u , we could determine analytically a threshold τ_u^* for the appearance of Hopf bifurcation (Figure 2). It depends on τ_u , μ , μ_u and η , which are respectively the threshold for the existence of \mathbf{S}_u , the mortality rates of immature and mature uninfected individuals and the velocity at which the carrying capacity is achieved. In turn, the bigger η the wider the range of τ wherein oscillations around \mathbf{S}_u are observed (Figure 3 and 4) as well as stability switch occurs earlier (i.e. for smaller τ values). Observe that during the transient time, damped oscillations are seen in one of the components of \mathbf{S}_u . Although, we could not prove analytically the occurrence of Hopf bifurcation for the equilibrium \mathbf{S}_{wu} , we could get oscillations around this equilibrium numerically (Figure 5).

For many arthropod-borne diseases such as Dengue, Zika, and others, vector control is the only available way to control the transmission of the disease to the human population. In this context, the threshold for the persistence of the disease depends on the ratio between the vector and the human population. As the mosquito infected with *Wolbachia* transmits the virus less than the wild mosquito, the increase in the population of infected mosquitoes with a good choice of bacterial strains (that promotes an increase of R_w), can make interesting the technique proposed in this paper for mosquito control.

Several studies have addressed the importance of temperature on the dynamics of infected mosquitoes, since the spread and quantity of bacteria on mosquito tissues are modulated by this abiotic factor [34, 35]. Reproduction, dispersal, mating behavior, bacterial inheritance and cytoplasmic incompatibility can be strongly affected by temperature variations in the field. In our model, we varied the parameters R_u and R_w to take into account the change in these factors which could lead to the extinction of one or both populations, or their coexistence.

Based on observations both in laboratories and in nature, [34, 35], there is evidence of oscillations in mosquito populations due to the variation in temperature. We showed in this paper that an increase in the duration of the aquatic phase (the delay), due to a decrease in temperature, for instance, gives one of the following two scenarios. In the first scenario, an increase in the delay leads to the extinction of the infected mosquito and the persistence of the uninfected one (with oscillations that are first damped and then become periodic for the uninfected mosquito). In the second scenario, an increase in the delay maintains the persistence of the two populations, with the appearance of damped oscillations which afterwards become periodic. The existence of periodic solutions can be rather simply understood from the mathematical point of view as produced by a Hopf bifurcation.

Finally, variation in temperature may make ineffective the use of *Wolbachia*-infected mosquito as a biological technique to reduce the population of wild mosquito. In addition, several types of infection adapted to different field conditions are necessary; besides, the right time for the release of infected mosquito to optimize the invasion and colonization of this population in an environment already occupied by the wild population is an important problem to be addressed. The present work may contribute to the study of the influence of abiotic factors on the temporal dynamics of mosquito population.

Acknowledgements. ASB thanks the scholarship from CAPES (Coordenação de Aperfeiçoamento de Pessoal de Nível Superior - Brasil) and CPF thanks grant 18/24058-1 from São Paulo Research Foundation (FAPESP). Part of this

work was developed during a sandwich period of ASB at INRIA (Institut National de Recherche en Informatique et en Automatique - France) supervised by M. Adimy.

REFERENCES

- [1] T. H. Ant, C. S. Herd, V. Geoghegan, A. A. Hoffmann, and S. P. Sinkins. The *Wolbachia* strain wAu provides highly efficient virus transmission blocking in *Aedes aegypti*. *PLoS Pathogens*, 14(1), 2018. doi: 10.1371/journal.ppat.1006815.
- [2] Z. A. Awraahman, F. Champion de Crespigny, and N. Wedell. The impact of *Wolbachia*, male age and mating history on cytoplasmic incompatibility and sperm transfer in *Drosophila simulans*. *Journal of Evolutionary Biology*, 27(1):1–10, 2014. doi:10.1111/jeb.12270.
- [3] J. K. Axford, P. A. Ross, H. L. Yeap, A. G. Callahan, and A. A. Hoffmann. Fitness of walbb *Wolbachia* infection in *Aedes aegypti*: parameter estimates in an outcrossed background and potential for population invasion. *The American Journal of Tropical Medicine and Hygiene*, 94(3):507–516, 2016. doi:10.4269/ajtmh.15-0608.
- [4] E. Beretta and Y. Kuang. Geometric stability switch criteria in delay differential systems with delay dependent parameters. *SIAM Journal on Mathematical Analysis*, 33(5):1144–1165, 2002. doi:10.1137/S0036141000376086.
- [5] L. Berezansky, E. Braverman, and L. Idels. Nicholson’s blowflies differential equations revisited: Main results and open problems. *Applied Mathematical Modelling*, 34(6):1405–1417, 2010. doi:10.1016/j.apm.2009.08.027.
- [6] L. Berezansky, L. Idels, and L. Troib. Global dynamics of nicholson-type delay systems with applications. *Nonlinear Analysis: Real World Applications*, 12(1):436–445, 2011. doi:10.1016/j.nonrwa.2010.06.028.
- [7] P.-A. Bliman, M. S. Aronna, F. C. Coelho, and M. A. H. B. da Silva. Ensuring successful introduction of *Wolbachia* in natural populations of *Aedes aegypti* by means of feedback control. *Journal of Mathematical Biology*, 76:1269–1300, 2018. doi:10.1007/s00285-017-1174-x.
- [8] P.-A. Bliman, D. Cardona-Salgado, Y. Dumont, and O. Vasilieva. Implementation of control strategies for sterile insect techniques. *Mathematical Biosciences*, 314:43–60, 2019. doi:10.1016/j.mbs.2019.06.002.
- [9] S. R. Bordenstein and S. R. Bordenstein. Temperature affects the tripartite interactions between bacteriophage WO, *Wolbachia*, and cytoplasmic incompatibility. *PLoS ONE*, 6(12), 2011. doi: 10.1371/journal.pone.0029106.
- [10] E. Braverman and D. Kinzbulatov. Nicholson’s blowflies equation with a distributed delay. *Canadian Applied Mathematics Quarterly*, 14(2):107–128, 2006.
- [11] R. A. Costello. *Effects of environmental and physiological factors on the acoustic behavior of Aedes aegypti (L.) (Diptera: Culicidae)*. PhD thesis, University of Manitoba, Canada, 1974.
- [12] C. Dye. Models for the population dynamics of the yellow fever mosquito, *Aedes aegypti*. *The Journal of Animal Ecology*, 53(1):247–268, 1984. doi:10.2307/4355.
- [13] J. Z. Farkas and P. Hinow. Structured and unstructured continuous models for *Wolbachia* infections. *Bulletin of Mathematical Biology*, 72:2067–2088, 2010. doi:10.1007/s11538-010-9528-1.
- [14] J. Z. Farkas, S. A. Gourley, R. Liu, and A. A. Yakubu. Modelling *Wolbachia* infection in a sex-structured mosquito population carrying west nile virus. *Journal of Mathematical Biology*, 75(3):621–647, 2017. doi:10.1007/s00285-017-1096-7.
- [15] C. P. Ferreira. *Aedes aegypti* and *Wolbachia* interaction: population persistence in a changing environment. *Theoretical ecology*, 2019. doi:10.1007/s12080-019-00435-9.
- [16] C. P. Ferreira, H. M. Yang, and L. Esteva. Assessing the suitability of sterile insect technique applied to *Aedes aegypti*. *Journal of Biological Systems*, 16(4):565–577, 2008. doi:10.1142/S0218339008002691.
- [17] D. J. Gubler. The global emergence/resurgence of arboviral diseases as public health problems. *Archives of Medical Research*, 33(4):330–342, 2002. doi:10.1016/s0188-4409(02)00378-8.
- [18] N. D. Hayes. Roots of the transcendental equation associated with a certain difference-differential equation. *Journal of the London Mathematical Society*, pages 226–232, 1950. doi:10.1112/jlms/s1-25.3.226.

- [19] S. P. Hernandez, A. M. Loaiza, and C. A. A. Minoli. A reaction-diffusion model for controlling the *Aedes aegypti* with *Wolbachia*. *International Journal of Contemporary Mathematical Sciences*, 11(8):385–394, 2016. doi:10.12988/ijcms.2016.511713.
- [20] A. A. Hoffmann, B. L. Montgomery, J. Popovici, I. Iturbe-Ormaetxe, P. H. Johnson, F. Muzzi, M. Greenfield, M. Durkan, Y. S. Leonga, Y. Dong, H. Cook, J. Axford, A. G. Callahan, N. Kenny, C. Omodei, E. A. McGraw, P. A. Ryan, S. A. Ritchie, M. Turelli, and S. L. O’Neill. Successful establishment of *Wolbachia* in *Aedes* populations to suppress dengue transmission. *Nature*, 476:454–457, 2011. doi:10.1038/nature10356.
- [21] M. Huang, M. X. Tang, and J. S. Yu. *Wolbachia* infection dynamics by reaction-diffusion equations. *Science China Mathematics*, 58(1):77–96, 2015. doi:10.1007/s11425-014-4934-8.
- [22] M. Huang, J. Luo, L. Hu, B. Zheng, and J. Yu. Assessing the efficiency of *Wolbachia* driven *Aedes* mosquito suppression by delay differential equations. *Journal of Theoretical Biology*, 440, 2018. doi:10.1016/j.jtbi.2017.12.012.
- [23] M. G. Huang, M. X. Tang, J. S. Yu, and Bo Zheng. The impact of mating competitiveness and incomplete cytoplasmic incompatibility on *Wolbachia*-driven mosquito population suppression. *Mathematical Biosciences and Engineering*, 16(5):4741–4757, 2019. doi:10.3934/mbe.2019238.
- [24] H. Hughes and N. Britton. Modelling the use of *Wolbachia* to control dengue fever transmission. *Bulletin of Mathematical Biology*, 75, 2013. doi:10.1007/s11538-013-9835-4.
- [25] L. Idels and M. Kipnis. Stability criteria for a nonlinear nonautonomous system with delays. *Applied Mathematical Modelling*, 33:2293–2297, 2009. doi:10.1016/j.apm.2008.06.005.
- [26] S. Lunel J. Hale. *Introduction to Functional Differential Equations*. Appl. Math. Sci., Springer-Verlag, 1993.
- [27] M. Keeling, F. M. Jiggins, and J. M. Read. The invasion and coexistence of competing *Wolbachia* strains. *Heredity*, 91(4):382–8, 2003. doi:10.1038/sj.hdy.6800343.
- [28] J. G. King, C. Souto-Maior, L. M. Sartori, R. M. de Freitas, and M. Gomes. Variation in *Wolbachia* effects on *Aedes* mosquitoes as a determinant of invasiveness and vectorial capacity. *Nature Communications*, 9, 2018. doi:10.1038/s41467-018-03981-8.
- [29] X. Ling, A. M. Carrie, T. Panpim, and M. H. James. Two-sex mosquito model for the persistence of *Wolbachia*. *Journal of Biological Dynamics*, 11:216–237, 2017. doi:10.1080/17513758.2016.1229051.
- [30] C. J. McMeniman, R. V. Lane, B. N. Cass, A. W. C. Fong, M. Sidhu, Y.-F. Wang, and S. L. O’Neill. Stable introduction of a life-shortening *Wolbachia* infection into the mosquito *Aedes aegypti*. *Science*, 323(5910):141–144, 2009.
- [31] M. Ndi, R. Hickson, and G. Mercer. Modelling the introduction of *Wolbachia* into *Aedes aegypti* mosquitoes to reduce dengue transmission. *The ANZIAM Journal*, 53(3):213–227, 2012. doi:10.1017/S1446181112000132.
- [32] Z. Qu, L. Xue, and J. Hyman. Modeling the transmission of *Wolbachia* in mosquitoes for controlling mosquito-borne diseases. *SIAM Journal on Applied Mathematics*, 78(2):826–852, 2018. doi:10.1137/17M1130800.
- [33] M. Rafikov, E. Rafikova, and H. M. Yang. Optimization of the *Aedes aegypti* control strategies for integrated vector management. *Journal of Applied Mathematics*, 2015. doi:10.1155/2015/918194.
- [34] J. M. Reinhold, C. R. Lazzari, and C. Lahondère. Effects of the environmental temperature on *Aedes aegypti* and *Aedes albopictus* mosquitoes: A review. *Insects*, 9(4), 2018. doi:10.3390/insects9040158.
- [35] P. A. Ross, I. Wiwatanaratnabutr, J. K. Axford, V. L. White, N. M. Endersby-Harshman, and A. A. Hoffmann. *Wolbachia* infections in *Aedes aegypti* differ markedly in their response to cyclical heat stress. *PLoS Pathogens*, 13(1), 2017. doi:10.1371/journal.ppat.1006006.
- [36] I. E. Leonard T. Hillen and H. Van Roessel. *Partial Differential Equations: Theory and Completely Solved Problems*. Wiley, 2012.
- [37] Z. Veneti, M. E. Clark, T. L. Karr, C. Savakis, and K. Bourtzis. Heads or tails: Host-parasite interactions in the *Drosophila-Wolbachia* system. *Applied and Environmental Microbiology*, 70(9):5366–5372, 2004. doi:10.1128/AEM.70.9.5366-5372.2004.

- [38] P. F. Viana-Medeiros, D. F. Bellinato, A. J. Martins, and D. Valle. Insecticide resistance, associated mechanisms and fitness aspects in two brazilian *Stegomyia aegypti* (= *Aedes aegypti*) populations. *Medical and Veterinary Entomology*, 31(4):340–350, 2017. doi:10.1111/mve.12241.
- [39] T. Walker, P. H. Johnson, L. A. Moreira, I. Iturbe-Ormaetxe, F. D. Frentiu, C. J. McMeniman, Y. S. Leong, Y. Dong, J. Axford, P. Kriesner, A. L. Lloyd, S. A. Ritchie, S. L. O’Neill, and A. A. Hoffmann. The wmel *Wolbachia* strain blocks dengue and invades caged *Aedes aegypti* populations. *Nature*, 475:450–453, 2011. doi:10.1038/nature10355.
- [40] Z. Xi, C. C. Khoo, and S. L. Dobson. *Wolbachia* establishment and invasion in an *Aedes aegypti* laboratory population. *Science*, 310(5746):326–328, 2005. doi:10.1126/science.1117607.
- [41] H. M. Yang and C. P. Ferreira. Assessing the effects of vector control on dengue transmission. *Applied Mathematics and Computation*, 198(1):401–413, 2008. doi:10.1016/j.amc.2007.08.046.
- [42] H. M. Yang, M. L. Macoris, K. C. Galvani, M. T. Andrighetti, and D. M. Wanderley. Assessing the effects of temperature on the population of *Aedes aegypti*, the vector of dengue. *Epidemiology and Infection*, 137(8):1188–1202, 2009. doi:10.1017/S0950268809002040.
- [43] H. L. Yeap, P. Mee, T. Walker, A. R. Weeks, S. L. O’Neill, P. Johnson, S. A. Ritchie, K. M. Richardson, C. Noteg, N. M. Endersby, and A. A. Hoffmann. Dynamics of the “Popcorn” *Wolbachia* infection in outbred *Aedes aegypti* informs prospects for mosquito vector control. *Genetics*, 187(2):583–595, 2011. doi:10.1534/genetics.110.122390.

Thermal Requirements and Population Viability of Soybean Looper (Lepidoptera: Noctuidae)

A. S. Benedito¹, O. A. Fernandes², and C. P. Ferreira¹

¹*Institute of Biosciences, São Paulo State University, Rua Prof. Dr. Antonio Celso Vagner Zanin, 250, 18618-689, Botucatu, SP, Brazil*

²*School of Agricultural and Veterinary Sciences, São Paulo State University, Access Road Prof. Paulo Donato Castellane, 14884-900, Jaboticabal, SP, Brazil*

Abstract

Development, mortality, fecundity and longevity of soybean looper *Chrysodeixis includens* (Lepidoptera: Noctuidae) were examined at six constant temperatures (18, 22, 25, 28, 32 and 36°C) under laboratory conditions. The development from egg to adult was completed between 18 and 32°C. Linear and nonlinear models were fitted to the data to estimate thermal constants and bioclimatic thresholds. Although the development of immature stages of *C. includens* can be expected across broader temperature ranges, this species is meant to complete the whole cycle and recover from low densities between 19.4 and 29.8°C. The best fitness is achieved at 25.2°C. The results can be used to parameterize phenological or mathematical models to forecast the occurrence of different stages of *C. includens* in the field and help optimize the efforts to control this insect-pest.

Keywords: thermal biology; life-history traits; intrinsic growth rate; pest control

Introduction

The soybean looper, *Chrysodeixis includens* (Walker, 1858) (Lepidoptera: Noctuidae, Plusiinae), is a lepidopteran pest geographically restricted to the Western Hemisphere (Herzog 1980, Alford and Hammond Jr 1982, Barrionuevo and San Blas 2016). It is a polyphagous defoliator whose larval stage lasts approximately two weeks (Smith et al. 1994) and can cause economically damaging losses to host plants (Herzog 1980). Although this insect feeds mainly on soybean, it is able to survive on different plant species of at least 28 botanical families such as cotton, tobacco, common bean and sunflower, which especially increases its importance for agriculture and integrated pest management (Herzog 1980, Specht et al. 2015, Moonga and Davis 2016).

Until 2003, *C. includens* was considered a minor pest of soybean in Brazil, because it was naturally controlled by parasitoids and entomopathogenic fungi (Specht et al. 2015). However, the introduction of soybean rust (*Phakopsora pachyrhizi* Syd. & P. Syd.) in 2001 led growers to apply fungicide in order to reduce losses and to assure production (Yorinori et al. 2005). A side effect of this application was the negative impact of fungicides on the naturally occurring entomopathogenic fungi *Metarhizium rileyi* which used to keep the population of *C. includens* under control (Sosa-Gómez et al. 2003). Consequently, the soybean looper became a key pest of soybean in the country (Bueno et al. 2009, Specht et al. 2015).

While in the USA *C. includens* is migratory in some parts of the territory due to extreme low temperatures (Herzog 1980), milder weather conditions and the year-round presence of crops theoretically favour the occurrence and abundance of polyphagous insects as it in the Brazilian Savanna. Nevertheless, its presence is hardly detected in most months and elevated abundances are restricted to a little part of the rainy season and practically synchronic to soybean availability (Santos et al. 2017, Zulin et al. 2018).

Temperature is perhaps the most important abiotic factor which affects insect dynamics. Its influence on the life-history traits of a species includes changes in fecundity, mortality and development rates, and mating behavior (Huffaker et al. 1999). Despite the aforementioned economic importance and extensive research on control methods for the soybean looper, the literature is scarce with regard to temperature influence on *C. includens*. For instance, Mason and Mack (1984) investigated the impact of temperature variation on oviposition rate and adult female longevity. On the other hand, Barrionuevo et al. (2012) determined life cycle, reproductive and population parameters, using only one constant temperature. Likewise, Specht et al. (2019) studied development, survival, reproduction and other traits of *C. includens* feeding on two different crops (soybean and forage turnip).

Understanding phenology of an insect species at different temperatures is crucial for predicting its seasonal occurrence and integrated management planing. In this context, many mathematical models describing insect developmental rate as a function of temperature are already proposed (Kontodimas et al. 2004, Aghdam et al. 2009). Linear models are widely used to explain the straight relationship between the developmental rate and temperature (in an intermediate range of temperature), and to calculate lower developmental thresholds and thermal constants required to complete development of immature stages (Campbell et al. 1974, Ikemoto and Takai 2000). In order to describe the developmental rate more realistically and over a wider temperature range, several nonlinear models have been applied to provide estimated values for optimum and maximum temperatures and also for minimum temperature for development (Kontodimas et al. 2004, Aghdam et al. 2009). Nonetheless, estimation of thermal constant cannot be derived from nonlinear models (Kontodimas et al. 2004, Aghdam et al. 2009).

In addition to these parameters, the intrinsic growth rate can be a useful metric to quantify populations

persistence by comparing the performance of populations inhabiting different environments. It is defined as the per capita growth rate of a population in the absence of density-dependent factors such as resource limitation and natural enemies. This parameter is particularly important in determining the ability of a species to recover from low densities, because density-dependent factors are less important at low densities than the intrinsic ability of the species to achieve a net increase in birth and developmental rates relative to death rates (Amarasekare and Savage 2012, Amarasekare and Coutinho 2013). If environmental conditions are such that the intrinsic growth rate cannot be positive at small population density, one would expect that the species will not be viable in such environment (Amarasekare and Savage 2012, Amarasekare and Coutinho 2013). Compared with other measures of population viability, a distinctive attribute of the intrinsic growth rate is that it incorporates not only survival and reproduction, but also development, and hence the effects of environmental factors on the entire life cycle of the target population (Amarasekare and Coutinho 2013). Thus, it is a particularly useful metric for assessing the viability of many ectothermic taxa having complex life cycles, enabling the estimation of a temperature range where it is feasible.

Therefore, the objectives of this study were: (i) to determine the thermal characteristics of *C. includens*, estimating the lower and upper temperature thresholds, and the optimal temperature for immature stages through linear and nonlinear temperature-driven models fitted to laboratory data, and (ii) to predict the species viability through the intrinsic growth rate which is evaluated as a function of the life-history traits of the population under different temperatures.

Materials and Methods

Soybean Looper Stock

Larvae of *C. includens* were obtained from a laboratory colony (Corteva Agrisciences, Mogi Mirim, SP, Brazil). They were kept in plastic cups (200 ml) and fed on artificial diet based on Greene et al. (1976) but using white bean as protein source. These plastic cups were maintained in climatic chambers ($25 \pm 1^\circ\text{C}$; $70 \pm 10\%$ RH and 12L:12D) until adult emergence. After emergence, adults were transferred into a Polyvinyl Chloride (PVC) cage (30 cm in diameter x 30 cm high) whose top was closed with voile fabric to allow ventilation. The cage was internally covered with white paper as substrate for oviposition. Adults were fed using cotton swabs soaked with 10% aqueous honey solution placed on the bottom of the cage. Eggs from F1, laid on the same date, and larvae from F2 generations were used in the experiments.

Data Collection

Rearing was conducted at six constant temperatures, 18, 22, 25, 28, 32 and 36°C in climate chambers. Photoperiod and relative humidity were maintained at 12L:12D and $70 \pm 10\%$, respectively.

For the egg study, a total of 600 eggs (< 24 h old) were distributed into the six temperatures (treatments) being 100 eggs per temperature placed into a Petri dish (1.5 cm high x 10 cm in diameter). Distilled water was sprinkled on the eggs daily every morning to avoid dissection. Egg development and mortality were monitored at each 24 hours and hatching date recorded.

For the larvae and pupae study, eggs were initially separated from the mating cage and placed in Petri dishes to allow embryo development at 25°C. After hatching, a total of 180 neonates larvae (< 24 h old) were transferred to individualized test tubes (8.5 cm high x 2.5 cm in diameter) containing artificial diet (Greene et al. 1976), being 30 larvae at each treatment. They were also monitored for development (including molting of all larval instars) and mortality at each 24 hours. After pupation, insects were kept in the same test tubes until adult emergence. Pupal viability was daily registered. Upon emergence, pupal cases were used for sex determination according to Butt and Cantu (1962). Adults emerged on the same day were separated to establish mating couples. Each couple was transferred into a plastic cup (200 ml) internally covered with white paper which was replaced daily. Daily oviposition and death of adults were recorded.

Linear Developmental Models

In order to estimate the linear relationship between temperature and development rate of *C. includens* two approaches were used. Both came from the *law of total effective temperatures* that assures the temperature-dependent development of ectotherms is expressed by:

$$K = D(T - T_{\min}), \quad (1)$$

where D is the duration of development (in days), T is temperature (in degrees Celsius), T_{\min} is the temperature threshold at which development is either zero or no measurable development occurs, and K is called species (or stage-specific) thermal constant, defined as the number of degree-days (DD) or heat units above the threshold required to achieve the next stage or maturation. Linear models work well when development is measured at intermediate temperature; at lower and upper temperature (extreme conditions) deviation from linearity is observed, and nonlinear models are more appropriate. By fitting equation (1) to laboratorial data of DT versus D , the parameters K (y intercept) and T_{\min} (slope coefficient) can be estimated (Ikemoto and Takai 2000).

Usually, a reciprocal transformation is carried out on the empirical data, and the equation (1) is rewritten

as:

$$\frac{1}{D} = \frac{T}{K} - \frac{T_{\min}}{K}. \quad (2)$$

From the plot of the development rate $r = 1/D$ versus T , the lower temperature threshold (T_{\min}) can be determined by the x -intercept method, i.e., by extrapolation of the regression line. In this case, the approximated standard errors (SE) of estimated T_{\min} and K are given by:

$$SE_{T_{\min}} = \frac{\bar{r}}{b} \sqrt{\frac{s^2}{n\bar{r}^2} + \left(\frac{SE_b}{b}\right)^2} \quad \text{and} \quad SE_K = SE_b/b^2,$$

where \bar{r} is the sample mean of r , s^2 is the residual mean square, b is the slope of the fitted straight line, i.e., $1/K$, SE_b is the standard error of b , and n is the sample size (Campbell et al. 1974).

Nonlinear Developmental Models

Seven published nonlinear (whether in their parameters or in their variables) models, commonly used for modeling arthropod development rates (Kontodimas et al. 2004, Aghdam et al. 2009), were used to fit individual development rate as a function of temperature (Table 1). The optimum (T_{opt}), lower (T_{\min}) and upper (T_{\max}) temperatures were obtained straightaway or indirectly from the models. T_{opt} is the threshold temperature at which developmental rate assumes its maximum value, while T_{\max} is the lethal threshold at which life cannot be maintained for a long time or the development ceases.

Intrinsic growth rate

Also known as Malthusian parameter, the intrinsic growth rate has been used as a measure of species fitness under temperature variation (Savage et al. 2004). Furthermore, it permits the estimation of the viable thermal range from T_{vmin} to T_{vmax} , the minimum and maximum viability temperature thresholds, respectively, where a complete development (from egg to adult) can occur, and the temperature T_{vopt} where the species growth rate is maximum. The intrinsic growth rate ξ as a function of the temperature is given by (Amarasekare and Savage 2012):

$$\xi(T) = -d(T) + \frac{1}{\phi(T)} W(b(T)\phi(T) \exp(d(T) - \bar{d}(T)\phi(T))), \quad (3)$$

where W represents the principal (positive) branch of the Lambert W function, and the functions $b(T)$, $d(T)$, $\bar{d}(T)$ and $\phi(T)$ are, respectively, the empirically measured temperature response function for the average per capita birth rate, adult mortality rate, immature mortality rate (all in days⁻¹) and the age (in days) at maturity. Equation (3) assumes a stable age distribution of the population and a constant age-specific rate

of death and reproduction. The reciprocal of average adult longevity yields an estimate of the per capita adult mortality rate. In turn, the per capita immature mortality rate is estimated by $\bar{d} = -\ln(s)/\tau$, where s is the immature survivorship (proportion of individuals that survived up adult stage) and τ is the average duration (in days) of immature stage (from egg to adult). Since the data of eggs and larvae do not come from the same generation, we multiplied the survivorship (by assuming it as survival probability) of eggs by that of larva up to adult stage to obtain s .

The per capita birth rate of most ectotherms exhibits a symmetric and unimodal response to temperature that is well-described by a Gaussian function:

$$b(T) = b_o e^{-\frac{(T-T_o)^2}{2\sigma^2}}, \quad (4)$$

where $b(T)$ is the average per capita birth rate at temperature T , b_o is the average per capita birth rate attained at an optimal temperature for oviposition T_o and σ is the standard deviation of the optimum. Mean lifetime fecundity divided by the average female longevity yielded a daily per capita birth rate at each temperature.

In general, the per capita mortality rate of ectotherms exhibits a monotonic temperature response that is well depicted by the Boltzmann–Arrhenius function for reaction kinetics (Savage et al. 2004). Nevertheless, some studies have found that mortality rates can increase at low temperatures (Morgan et al. 2001). Thus, we used a second degree polynomial function to describe the temperature response of juvenile and adult mortality rates:

$$\mu(T) = aT^2 + bT + c, \quad (5)$$

where $\mu := \mu(T)$ is the immature (\bar{d}) or adult (d) mortality rate at temperature T , and a , b and c are model parameters.

Ectotherm developmental rates exhibit a left-skewed temperature response that results from the reduction in reaction rates at low and high temperature extremes due to enzyme inactivation (Amarasekare and Coutinho 2013). Thus, in order to describe the temperature response of age at maturity (time spend in developing from egg to mature adult), we used the Brière-1 model:

$$\frac{1}{\phi(T)} = aT (T - \bar{T}_{\min}) \sqrt{\bar{T}_{\max} - T}, \quad (6)$$

where $\phi(T)$ is the age at maturity, \bar{T}_{\min} and \bar{T}_{\max} are respectively the minimum and maximum temperature thresholds, between which the development up to the adult maturity can be achieved.

The models (4), (5) and (6) were fitted to the laboratory data in order to calculate $\xi(T)$ through equation

(3). Juvenile mortality and age at maturity values were obtained by combining data from the different immature stages. Afterwards, the lower and upper temperature thresholds T_{vmin} and T_{vmax} were obtained by setting the right-hand side of equation (3) to zero and solving it numerically for T .

Statistical Analysis

For all linear and nonlinear regressions performed, it is assumed that the variability of the experimental error (differences between units) is estimated by the variability between individual responses at the same temperature. Errors were checked for normality by using the Kolmogorov-Smirnov and Shapiro-Wilk tests. A few points (no more than three) at low and high temperatures for each immature stage have been shown to be influential in the residual analysis, but excluding them was not justified.

The effect of temperature on the developmental time of soybean looper immature stages and longevity was analyzed by using one-way analysis of variance (ANOVA) at $\alpha = 0.05$. Means were separated by using the Tukey-Kramer honestly significant difference (HSD) test.

The performance of linear developmental models was compared through their values of the coefficient of determination R^2 . Nonlinear developmental model evaluation was made based on both goodness-of-fit and biological significance of estimated values of the bioclimatic thresholds. Since there is no well-defined R^2 statistic (calculated here as the squared correlation coefficient between fitted values and data) for nonlinear models, and the residual sum of squares (RSS) do not provide good discrimination between models with different number of parameters, we used the Akaike information criterion (AIC), which is parameter independent, to assess goodness-of-fit of the nonlinear models and establish their statistical rank. It is defined as $AIC = n \ln(RSS/n) + 2p$, where n is the number of observations and p is the number of model parameters. Better fits were associated to smaller values of AIC.

All statistical analyses were conducted using R version 3.6.1 (R Core Team 2019) in RStudio version 1.2.5001 (RStudio Team 2019) .

Results

Temperature Range for Development

At 36°C, the eggs did not hatch and no larvae survived to pupate. Consequently, this temperature was removed from all analysis. In the temperature range of 18 – 32°C, the insect was able to complete its development.

Survivorship, Longevity and Fecundity

The egg stage presented the lowest survivorship compared to other immature stages despite the temperatures (Table 2). Larval survivorship decreased substantially at 32°C, whereas pupae were mainly affected at 18°C. Overall, the survivorship of immature stages increased on the range of temperature between 18 and 25°C, and decreased beyond the latter. One-way ANOVA showed a significant effect of temperature on longevity of soybean looper ($p < 0.0001$). The longest lifespan of adults was observed at 22 and 25°C. The extreme temperatures evaluated (18 and 32°C) caused reduction of more than 40% on the longevity (Table 3). The largest fecundity was obtained at 25°C and sharp decreasing was observed at lower or higher temperatures. At 32°C few adults emerged and, therefore, only few couples were formed. However, oviposition was not observed at this temperature (Table 3).

Development Time

One-way ANOVA also showed a significant effect of temperature on developmental time for all soybean looper immature life stages ($p < 0.0001$). The duration of development decreased with increasing in temperature for the larval stage; but more strictly for egg and pupa this trend occurred solely until 28°C. Development of eggs, larvae and pupae varied from 2 (25, 28 and 32°C) to 8 days (18°C); 10 (32 °C) to 49 days (18 °C); and 5 (28 °C) to 23 days (18 °C), respectively. Taking into consideration the duration of all immature stages, the life cycle (egg to adult) of *C. includens* varied, on average, from 22.10 (32 °C) to 62.16 days (18 °C). However, it is important to highlight that the mean development period for 18 and 32°C was obtained based on few specimens (6 and 7, respectively) surviving up to the adult stage.

Developmental Models

A linear relationship between developmental rate and temperature was observed in the range between 18 and 28°C for each immature stage (Table 4). However, outside this range, developmental rates deviate from the straight line and the temperature of 32°C was therefore excluded from the analysis, as suggested by Ikemoto and Takai (2000) and Kontodimas et al. (2004). As expected, this linear relationship for all immature stages was better explained by the approach proposed by Ikemoto and Takai (2000), i.e. equation (1), with greater R^2 coefficient and lower p-values. According to this model, T_{\min} was between 13.12 ± 0.32 and $14.75 \pm 0.28^\circ\text{C}$ for the immature stages, and the time required to complete physiological development (=thermal constant) of eggs, larvae and pupae were respectively 35.4 ± 2.5 , 181.8 ± 7.1 and 88.6 ± 3.2 DD.

All nonlinear models (Table 5) fitted the development rate as a function of temperature of larva and pupa of *C. includens* (Fig. 1). However, since the chosen scaling (days) was very long to successfully catch

nonlinearities in the developmental rate variation of eggs, analysis for this stage was not performed. A wide variation among the models in estimating the values of thermal requirements was observed. At the end, only two models were retained for each immature analyzed stage, because their values are in agreement with what is expected from biology (Table 6). The Brière-1 model presented the most reasonable estimates of upper threshold (T_{\max}) compared to Equation-16 in terms of overestimation. The minimum (T_{\min}), maximum (T_{\max}) and optimum (T_{opt}) temperature thresholds for the larval stage were 10.7, 32.1 and 38.6°C, respectively. For the pupal stage the estimated values were 15.6, 30.3 and 35.3°C, respectively.

Intrinsic Growth Rate

Explicit temperature dependence of fecundity, mortality and development rate were considered by fitting models (4)-(6) to empirical data. Birth rate decreases at extreme temperatures, and reaches the highest value at 25.54°C (75.69 eggs/female/day) (Fig. 2a). Immature and adult mortality rates increase at extreme temperatures presenting both a minimum mean value of mortality rate between 22 and 25°C (Fig. 2b,c). Finally, age at maturity decreases nonlinearly as temperature increases (Fig. 2d); for it the preoviposition period was not computed because there were not enough adult couples to assure sufficient and reliable data out of the range between 22 and 28°C. From the intrinsic growth rate curve (Fig. 2e), obtained by the equation (3), we found that the thermal tolerance of *C. includens* viability ranges from 19.4 to 29.8°C, being the optimum fitness at 25.2°C ($\xi = 0.191$).

Discussion

The present study is the first report of lower and upper threshold temperatures, thermal constant and optimal temperature for soybean looper *C. includens*. These parameters are crucial in mathematical and phenological models to better predict population dynamics of insects. Moreover, we calculated the intrinsic growth rate dependent on the life-history traits as a measure for the population viability of this species. For this, temperature response data of development, mortality, fecundity and longevity were obtained under laboratory conditions.

Clearly, temperature significantly affected the development of *C. includens*. The development time obtained for egg and pupal stages at 28°C in our study is slightly lower than the result reported by Barrionuevo et al. (2012), who reared this species in artificial diet and controlled environment (27 ± 2°C, 70-75% RH and 14:10 L:D). On the other hand, the development of larval stage observed by Barrionuevo et al. (2012) was almost twice as long (76%). This might be related to the influence of different types of nutrients in the diet provided to larvae (Andrade et al. 2016). As to 25°C, the development time for all immature stages is

absolutely consistent with Specht et al. (2019).

The immature survivorship was considerably lower for eggs whereas it was mildly higher for larvae and far greater for pupal stage in our study compared to those of Barrionuevo et al. (2012). Regarding to Specht et al. (2019), the remarkable difference in survivorship occurred for eggs while it was too close for larval and pupal stage. It is interesting to highlight that larvae and pupae seem to have larger thermal plasticity than eggs (Moghadam et al. 2019).

Considering the maximum estimated value for the lower temperature threshold, the development up to adult stage of this insect-pest is meant to be expected above 15.6°C (Brière-1 model). This strongly agrees with Tingle and Mitchell (1977) who registered in field significant adult activity, continuous reproduction and development of *C. includens* in the state of Florida, USA, exactly until this temperature. The values obtained for T_{\min} using the Brière-1 model (10.7 – 15.6°C) for larval and pupal stages seem to be the most reasonable (Table 6) and compatible with those of Ikemoto and Takay. Jarosik et al. (2011) suggested to use closely related species that share similar thermal requirements if information on the target species is lacking. The minimum temperature value for development obtained in our study corroborates the statement proposed by Jarosik et al. (2011), once the values reported by Garcia et al. (2018) for *Spodoptera frugiperda* (Lepidoptera: Noctuidae) (from 11.7 ± 1.2 to $14.1 \pm 0.9^\circ\text{C}$ at 14L:10D photoperiod and $70\% \pm 10\%$ RH) and by Mironidis and Savopoulou-Soultani (2008) for *Helicoverpa armigera* (Lepidoptera: Noctuidae) (from 10.17 to 11.95°C at 16L:8D photoperiod and $\geq 60\%$ RH) were within the range estimated.

As 36°C was deleterious for eggs of *C. includens* and all larvae died before completing development, we can conclude that all nonlinear models overestimated T_{\max} for the larval stage. This is probably because the lack of data at high temperatures (between 32 and 36°C) does not allow a good estimation of T_{\max} . Future experiments using development response to temperature should consider to obtain more data points in the range between 32 and 36°C, where it seems that the true maximum effective temperature lies. The optimal temperatures for immature stages 32.1 (larva) and 30.3°C (pupa), by Brière-1 model, was consistent with those of any other nonlinear model.

The intrinsic growth rate provides a complete cycle (egg to egg) temperature response for the species, and it is a quantitative measure of temperature response of species fitness. This parameter requires information about immature and adult stage such as surviving, development and fecundity. Overall, for *C. includens*, immature mortality rate had a greater sensitivity to temperature when compared to adult mortality rate, and both increased at extreme temperatures. The high pronounced peak observed for fecundity along with low variability around its maximum value is characteristic of tropical species (Amarasekare and Savage 2012). It is not clear if the lack of symmetry on the curve of the birth rate is associated to the fact that few adult couples were formed at 18 and 32°C or if this curve is really left skewed. The low availability of reproduction data at

these temperatures could imply overestimation of the lower threshold ($T_{vmin} = 19.4^{\circ}\text{C}$) and underestimation of the upper threshold ($T_{vmax} = 29.8.4^{\circ}\text{C}$) for *C. includens* viability. According to Amarasekare and Savage (2012), the width of the temperature response of birth rate has a strong effect on the proximity of T_{vmin} and T_{vmax} . Therefore, from this work, it is reasonable to assert that the temperature interval into which the overall cycle of *C. includens* is feasible shall not be narrower than the range between 19.4 and 29.8°C, where the species can survive, reproduce and develop. Thus, this species is meant to be found year-round in regions where annual temperature average is in this range. Furthermore, as cited above, the preoviposition period was not computed in the age maturity curve because of lacking data out of the intermediate temperature range.

Although the development of immature stages of *C. includens* can be expected across broader temperature ranges, this species seems able to complete its cycle and to recover from low densities in a narrower interval. Moreover, the intrinsic growth rate also illustrates the speed at which population recovering takes place. For *C. includens*, the highest values of ξ are observed around 25°C, which is consistent with population outbreaks observed in Brazilian soybean (Specht et al. 2015). In addition, the intrinsic growth rate allows exploring how much a species is likely to be impacted by perturbations to their thermal environments, and hence predicting extinction risk due to climate warming (Amarasekare and Savage 2012).

The results provided in the present work might be used to construct explicitly temperature-dependent models seeking to forecast accurately the occurrence of different stages of *C. includens* in field and help optimize the efforts of controlling this insect-pest.

Acknowledgements

The authors thank Éllen Rimkevicius Carbognin for rearing assistance, Luzia Aparecida Trinca for guidance in statistical analysis and Corteva Agriscience, Mogi Mirim, SP, Brazil for providing the insects. This work was financially supported in part by CAPES (Coordenação de Aperfeiçoamento de Pessoal de Nível Superior – Brasil) - Finance Code 001. CPF thanks grant 18/24058-1 from São Paulo Research Foundation (FAPESP).

References

- Aghdam, H. R., Y. Fathipour, G. Radjabi, and M. Rezapanah. 2009.** Temperature-dependent development and temperature thresholds of codling moth (Lepidoptera: Tortricidae) in Iran. *Environ. Entomol.* 38: 885–895.
- Alford, A. R. and A. M. Hammond Jr. 1982.** Plusiinae (Lepidoptera: Noctuidae) populations in Louisiana soybean ecosystems as determined with loop lure-baited traps. *J. Econ. Entomol.* 75: 647–657.
- Amarasekare, P. and R. M. Coutinho. 2013.** The intrinsic growth rate as a predictor of population viability under climate warming. *J. App. Ecol.* 82(6): 1240–1253.
- Amarasekare, P. and V. Savage. 2012.** A framework for elucidating the temperature dependence of fitness. *Am. Nat.* 179(2): 178–191.
- Analytis, S. 1981.** Relationship between temperature and development times in phytopathogenic fungus and in plant pests: a mathematical model. *Agric. Res.* 5: 133–159.
- Andrade, K., A. Bueno, D. M. da Silva, C. Stecca, A. Pasini, and M. C. N. de Oliveira. 2016.** Bioecological characteristics of *Chrysodeixis includens* (Lepidoptera: Noctuidae) fed on different hosts. *Austral Entomol.* 55(4): 449–454.
- Barrionuevo, M. J., M. G. Murúa, L. Goane, R. L. Meagher, and F. V. Navarro. 2012.** Life table studies of *Rachiplusia nu* (Guenée) and *Chrysodeixis* (= *Pseudoplusia*) *Includens* (Walker) (Lepidoptera: Noctuidae) on artificial diet. *Fla. Entomol.* 95(4): 944–951.
- Barrionuevo, M. J. and G. San Blas. 2016.** Redescription of immature stages of the soybean looper (Lepidoptera: Noctuidae: Plusiinae). *Can. Entomol.* 148(3): 247–259.
- Brière, J.-F., P. Pracros, A.-Y. Le Roux, and J.-S. Pierre. 1999.** A novel rate model of temperature-dependent development for arthropods. *Environ. Entomol.* 28: 22–29.
- Bueno, R. C. O. F., J. R. P. Parra, A. F. Bueno, and M. L. Haddad. 2009.** Desempenho de tricogramatídeos como potenciais agentes de controle de *Pseudoplusia includens* Walker (Lepidoptera: Noctuidae). *Neotrop. Entomol.* 38: 389–394.
- Butt, B. and E. Cantu. 1962.** Sex determination of lepidopterous pupae. U.S. Dept. of Agriculture ARS 33-75: 7p.
- Campbell, A., B. D. Frazer, N. Gilbert, A. P. Gutierrez, and M. Mackauer. 1974.** Temperature requirements of some aphids and their parasites. *J. App. Ecol.* 11(2): 431–438.

- Garcia, A., W. Godoy, J. Thomas, R. Nagoshi, and R. Meagher. 2018.** Delimiting strategic zones for the development of fall armyworm (Lepidoptera: Noctuidae) on corn in the state of Florida. *J. Econ. Entomol.* 111(1): 120–126.
- Greene, G., N. Leppla, and W. Dickerson. 1976.** Velvetbean caterpillar: a rearing procedure and artificial medium. *J. Econ. Entomol.* 69: 487–488.
- Harcourt, D. G. and J. M. Yee. 1982.** Polynomial algorithm for predicting the duration of insect life stages. *Environ. Entomol.* 11(3): 581–584.
- Herzog, D. C. 1980.** Sampling Soybean Looper on Soybean, pp. 141–168. In M. Kogan and D. Herzog (eds.), *Sampling methods in soybean entomology*. Springer, New York, NY.
- Huffaker, C. B., A. A. Berryman, and P. Turchin. 1999.** Dynamics and regulation of insect populations, pp. 269–305. In C. B. Huffaker and A. P. Gutierrez (eds.), *Ecological Entomology*. Wiley, New York.
- Ikemoto, T. and K. Takai. 2000.** A new linearized formula for the law of total effective temperature and the evaluation of line-fitting methods with both variables subject to error. *Environ. Entomol.* 29(4): 671–682.
- Jarosik, V., A. Honel, R. Magarey, and J. Skuhrovec. 2011.** Developmental database for phenology models: related insect and mite species have similar thermal requirements. *J. Econ. Entomol.* 104(6): 1870–1876.
- Kontodimas, D., P. Eliopoulos, G. J. Stathas, and L. Economou. 2004.** Comparative temperature-dependent development of *Nephus includens* (Kirsch) and *Nephus bisignatus* (Boheman) (Coleoptera: Coccinellidae) preying on *Planococcus citri* (Risso) (Homoptera: Pseudococcidae): evaluation of a linear and various nonlinear models using specific criteria. *Environ. Entomol.* 33: 1–11.
- Lactin, D., N. Holliday, D. Johnson, and R. Craigen. 1995.** Improved rate model of temperature-dependent development by arthropods. *Environ. Entomol.* 24: 68–75.
- Mason, L. and T. Mack. 1984.** Influence of temperature on oviposition and adult female longevity for the soybean looper *Pseudoplusia includens* Lepidoptera Noctuidae. *Environ. Entomol.* 13(2): 379–383.
- Mironidis, G. and M. Savopoulou-Soultani. 2008.** Development, survivorship, and reproduction of *Helicoverpa armigera* (Lepidoptera: Noctuidae) under constant and alternating temperatures. *Environ. Entomol.* 37(1): 16–28.

- Moghadam, N., T. Ketola, C. Pertoldi, S. Bahrndorff, and T. Kristensen. 2019.** Heat hardening capacity in *Drosophila melanogaster* is life stage-specific and juveniles show the highest plasticity. *Bio. Lett.* 15(2).
- Moonga, M. and J. Davis. 2016.** Partial life history of *Chrysodeixis includens* (Lepidoptera: Noctuidae) on summer hosts. *J. Econ. Entomol.* 109(4): 1713–1719.
- Morgan, D., K. Walters, and J. Aegerter. 2001.** Effect of temperature and cultivar on pea aphid, *Acyrtosiphon pisum* (Hemiptera: Aphididae) life history. *Bull. Entomol. Res.* 91: 47–52.
- R Core Team. 2019.** R: A Language and Environment for Statistical Computing. R Foundation for Statistical Computing, Vienna, Austria.
- RStudio Team. 2019.** RStudio: Integrated Development Environment for R. RStudio, Inc. Boston, MA.
- Santos, S. R. d., A. Specht, E. Carneiro, S. V. d. Paula-Moraes, and M. M. Casagrande. 2017.** Interseasonal variation of *Chrysodeixis includens* (Walker, [1858]) (Lepidoptera: Noctuidae) populations in the Brazilian Savanna. *Rev. Bras. Entomol.* 61: 294 – 299.
- Savage, V. M., J. F. Gillooly, J. H. Brown, G. B. West, and E. L. Charnov. 2004.** Effects of body size and temperature on population growth. *Am. Nat.* 163(3): 429–441.
- Smith, R., B. Freeman, and W. Foshee. 1994.** Soybean loopers: late season foliage feeders on cotton. Alabama Cooperative Extension Service. ANR-843.
- Sosa-Gómez, D. R., K. E. Delpin, F. Moscardi, and M. de H. Nozaki. 2003.** The impact of fungicides on *Nomuraea rileyi* (Farlow) Samson epizootics and on populations of *Anticarsia gemmatalis* Hübner (Lepidoptera: Noctuidae), on soybean. *Neotrop. Entomol.* 32: 287–291.
- Specht, A., S. V. de Paula-Moraes, and D. R. Sosa-Gómez. 2015.** Host plants of *Chrysodeixis includens* (Walker) (Lepidoptera, Noctuidae, Plusiinae). *Rev. Bras. Entomol.* 59(4): 343–345.
- Specht, A., D. R. Sosa-Gómez, V. F. Roque-Specht, E. Valduga, F. Gonzatti, S. M. Schuh, and E. Carneiro. 2019.** Biotic potential and life tables of *Chrysodeixis includens* (Lepidoptera: Noctuidae), *Rachiplusia nu*, and *Trichoplusia ni* on soybean and forage turnip. *J. Insect Sci.* 19(4): 1–8.
- Taylor, F. 1981.** Ecology and evolution of physiological time in insects. *Am. Nat.* 117(1): 1–23.
- Tingle, F. C. and E. R. Mitchell. 1977.** Seasonal populations of armyworms and loopers at Hastings, Florida. *Fla. Entomol.* 60(2): 115–122.

Yorinori, J. T., W. M. Paiva, R. D. Frederick, L. M. Costamilan, P. F. Bertagnolli, G. E. Hartman, C. V. Godoy, and J. Nunes. 2005. Epidemics of soybean rust (*Phakopsora pachyrhizi*) in Brazil and Paraguay from 2001 to 2003. *Plant Dis.* 89(6): 675–677.

Zulin, D., C. Avila, and E. Schlick-Souza. 2018. Population Fluctuation and Vertical Distribution of the Soybean Looper (*Chrysodeixis includens*) in Soybean Culture. *Am. J. Plant Sci.* 09: 1544–1556.

Tables and Figures

Table 1. Nonlinear (in parameters or variables) models fitted to development rate of larval and pupal stages of *C. includens* as a function of temperature.

| Model | Equation | Reference |
|---------------------------|---|--------------------------|
| Brière-1 | $r(T) = aT(T - T_{\min})(T_{\max} - T)^{\frac{1}{2}}$ | Brière et al. (1999) |
| Harcourt | $r(T) = a_0 + a_1T + a_2T^2 + a_3T^3$ | Harcourt and Yee (1982) |
| Equation-16 | $r(T) = a(T - T_{\min})^2(T_{\max} - T)$ | Kontodimas et al. (2004) |
| Pradhan-Taylor (Gaussian) | $r(T) = R_m \exp\left[-\frac{1}{2}\left(\frac{T - T_m}{T_\sigma}\right)^2\right]$ | Taylor (1981) |
| Logan-6/Lactin-1 | $r(T) = e^{\rho T} - e\left(\rho T_{Max} - \frac{T_{Max} - T}{\Delta}\right)$ | Lactin et al. (1995) |
| Logan-6/Lactin-2 | $r(T) = e^{\rho T} - e\left(\rho T_{Max} - \frac{T_{Max} - T}{\Delta}\right) + \lambda$ | Lactin et al. (1995) |
| Janisch/Analytis | $r(T) = \frac{2C}{a^{(T-T_m)} + b^{(T_m-T)}}$ | Analytis (1981) |

Table 2. Percent survival, minimum, maximum and mean developmental time of each immature stage of *C. includens* at five constant temperatures. The number of individuals at the beginning of each treatment is indicated between parenthesis near the temperature value.

| Stage | Temperature (°C) | Survival (%) | Developmental time (days) | | |
|-------|---------------------|-----------------|---------------------------|---------|-------------------|
| | | | Minimum | Maximum | Mean \pm SE |
| Egg | 18 (100) | 10.0 | 5 | 8 | 6.40 \pm 0.40a |
| | 22 (100) | 22.0 | 3 | 5 | 4.05 \pm 0.14b |
| | 25 (100) | 44.0 | 2 | 5 | 3.41 \pm 0.10c |
| | 28 (100) | 27.0 | 2 | 4 | 2.85 \pm 0.10d |
| | 32 (100) | 10.0 | 2 | 4 | 2.90 \pm 0.18cd |
| Larva | 18 (30) | 70.0 | 30 | 49 | 34.43 \pm 1.17a |
| | 22 (30) | 76.7 | 18 | 24 | 20.33 \pm 0.32b |
| | 25 (30) | 90.0 | 13 | 24 | 15.12 \pm 0.47c |
| | 28 (30) | 83.3 | 12 | 23 | 13.19 \pm 0.41c |
| | 32 (30) | 23.3 | 10 | 19 | 12.20 \pm 1.17c |
| Pupa | 18 (21) | 28.6 | 17 | 23 | 21.33 \pm 0.95a |
| | 22 (27) | 96.3 | 12 | 19 | 12.89 \pm 0.25b |
| | 25 (24) | 100.0 | 8 | 10 | 9.04 \pm 0.15c |
| | 28 (26) | 96.1 | 5 | 7 | 6.36 \pm 0.11d |
| | 32 (10) | 70.0 | 6 | 8 | 7.00 \pm 0.31d |

At each stage, means followed by the same letter are not significantly different at $\alpha = 0.05$ (Tukey-Kramer HSD test).

Table 3. Minimum, maximum and mean longevity (in days) of *C. includens*, and fecundity of adults at five constant temperatures. The number of couples at each treatment is indicated between parenthesis near the female mean longevity.

| Temperature (°C) | Longevity | | | | Fecundity \pm SE (eggs per female) |
|---------------------|-----------|---------|--------------------|-------------------------------------|---|
| | Minimum | Maximum | Mean \pm SE | Female (from couples) mean \pm SE | |
| 18 | 3 | 11 | 6.33 \pm 1.30bc | 11 (1) | 268.0 |
| 22 | 3 | 17 | 10.22 \pm 0.74ab | 10.83 \pm 0.78a (13) | 163.46 \pm 44.61 |
| 25 | 2 | 18 | 11.26 \pm 0.98a | 11.45 \pm 1.38a (11) | 835.09 \pm 243.52 |
| 28 | 2 | 15 | 5.84 \pm 0.61c | 4.82 \pm 0.44b (11) | 168.16 \pm 97.12 |
| 32 | 1 | 7 | 3.57 \pm 0.78c | 2.33 \pm 0.88b (3) | 0.0 |

Means followed by the same letter are not significantly different at $\alpha = 0.05$ (Tukey-Kramer HSD test)

Table 4. Linear regression, lower temperature threshold (T_{\min}) and thermal constant (K) (with approximated 95% confidence intervals) of immature stages of *C. includens*.

| Linear model | Stage | Linear equation | T_{\min} (°C) | K (DD) | R^2 | p |
|---------------|-------|-------------------------|----------------------|----------------------|--------|-----------|
| Campbell | Egg | $r = -0.1835 + 0.0196T$ | 9.37 (6.26, 12.48) | 51.1 (40.7, 61.4) | 0.4816 | 4.396e-16 |
| | Larva | $r = -0.0566 + 0.005T$ | 11.70 (10.79, 12.61) | 206.8 (191.5, 222.2) | 0.8795 | < 2.2e-16 |
| | Pupa | $r = -0.1843 + 0.0121T$ | 15.28 (14.60, 15.96) | 82.9 (77.1, 88.8) | 0.9075 | < 2.2e-16 |
| Ikemoto-Takai | Egg | $DT = 35.4 + 14.14D$ | 14.14 (12.83, 15.43) | 35.4 (30.4, 40.4) | 0.8223 | < 2.2e-16 |
| | Larva | $DT = 181.8 + 13.12D$ | 13.12 (12.48, 13.76) | 181.8 (167.7, 195.8) | 0.9449 | < 2.2e-16 |
| | Pupa | $DT = 88.6 + 14.75D$ | 14.75 (14.19, 15.31) | 88.6 (82.4, 94.9) | 0.9722 | < 2.2e-16 |

Table 5. Criteria values of goodness-of-fit for nonlinear models. The lower the AIC value, the higher the statistical rank. The models were adjusted to data of development rate versus temperature for larval and pupal stages of *C. includens*.

| Model | Larva | | | Pupa | | |
|---------------------------|--------|---------|------|--------|---------|------|
| | R^2 | AIC | Rank | R^2 | AIC | Rank |
| Brière-1 | 0.8383 | -720.96 | 2 | 0.8711 | -498.19 | 4 |
| Harcourt | 0.8348 | -711.88 | 6 | 0.9057 | -519.61 | 2 |
| Equation-16 | 0.8388 | -721.25 | 1 | 0.8695 | -493.33 | 5 |
| Pradhan-Taylor (Gaussian) | 0.8382 | -720.90 | 3 | 0.8848 | -504.17 | 3 |
| Logan-6/Lactin-1 | 0.8363 | -719.60 | 4 | 0.8139 | -465.86 | 6 |
| Logan-6/Lactin-2 | 0.8383 | -718.97 | 5 | 0.8142 | -463.99 | 7 |
| Janisch/Analytis | 0.8297 | -710.64 | 7 | 0.9089 | -528.72 | 1 |

Table 6. Parameter-values (with 95% confidence intervals) and bioclimatic thresholds for selected nonlinear temperature-driven rate models fitted to developmental rate of larval and pupal stages of *C. includens* based on statistical rank and biological significance.

| Stage | Model | Rank | Model parameter | Estimate | Bioclimatic Threshold | Computed value ^a |
|-------|-------------|------|-----------------|---|-----------------------|-----------------------------|
| Larva | Brière-1 | 2 | a | 4.95×10^{-5} (3.74×10^{-5} , 6.16×10^{-5}) | T_{\min} | 10.7 |
| | | | T_{\min} | 10.68 (8.62, 12.73) | T_{opt} | 32.1 |
| | | | T_{\max} | 38.59 (35.98, 41.20) | T_{\max} | 38.6 |
| | Equation-16 | 1 | a | 1.16×10^{-5} (6.12×10^{-6} , 1.70×10^{-5}) | T_{\min} | 8.3 |
| | | | T_{\min} | 8.34 (6.43, 10.25) | T_{opt} | 33.1 |
| | | | T_{\max} | 45.43 (40.60, 50.26) | T_{\max} | 45.4 |
| Pupa | Brière-1 | 4 | a | 1.58×10^{-4} (1.35×10^{-4} , 1.81×10^{-4}) | T_{\min} | 15.6 |
| | | | T_{\min} | 15.56 (14.64, 16.49) | T_{opt} | 30.3 |
| | | | T_{\max} | 35.30 (34.35, 36.26) | T_{\max} | 35.3 |
| | Equation-16 | 5 | a | 6.60×10^{-5} (4.69×10^{-5} , 8.51×10^{-5}) | T_{\min} | 13.5 |
| | | | T_{\min} | 13.50 (12.49, 14.50) | T_{opt} | 30.3 |
| | | | T_{\max} | 38.76 (37.14, 40.37) | T_{\max} | 38.8 |

^a An analytical expression to calculate the optimal temperature was derived from the models.

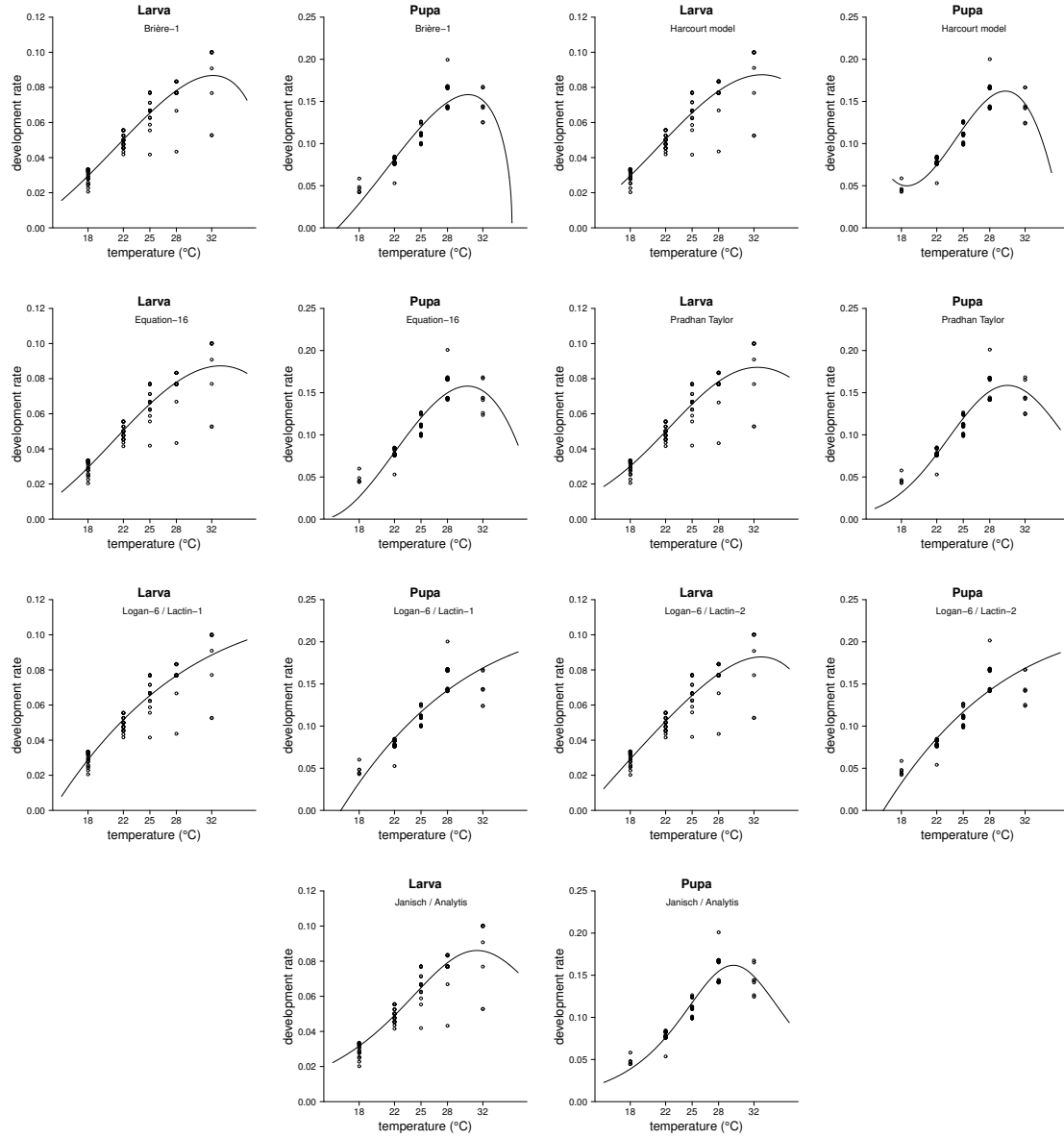


Fig. 1. Selected nonlinear temperature-driven rate models fitted to developmental rate of larval and pupal stages of *C. includens* based on statistical rank and biological significance.

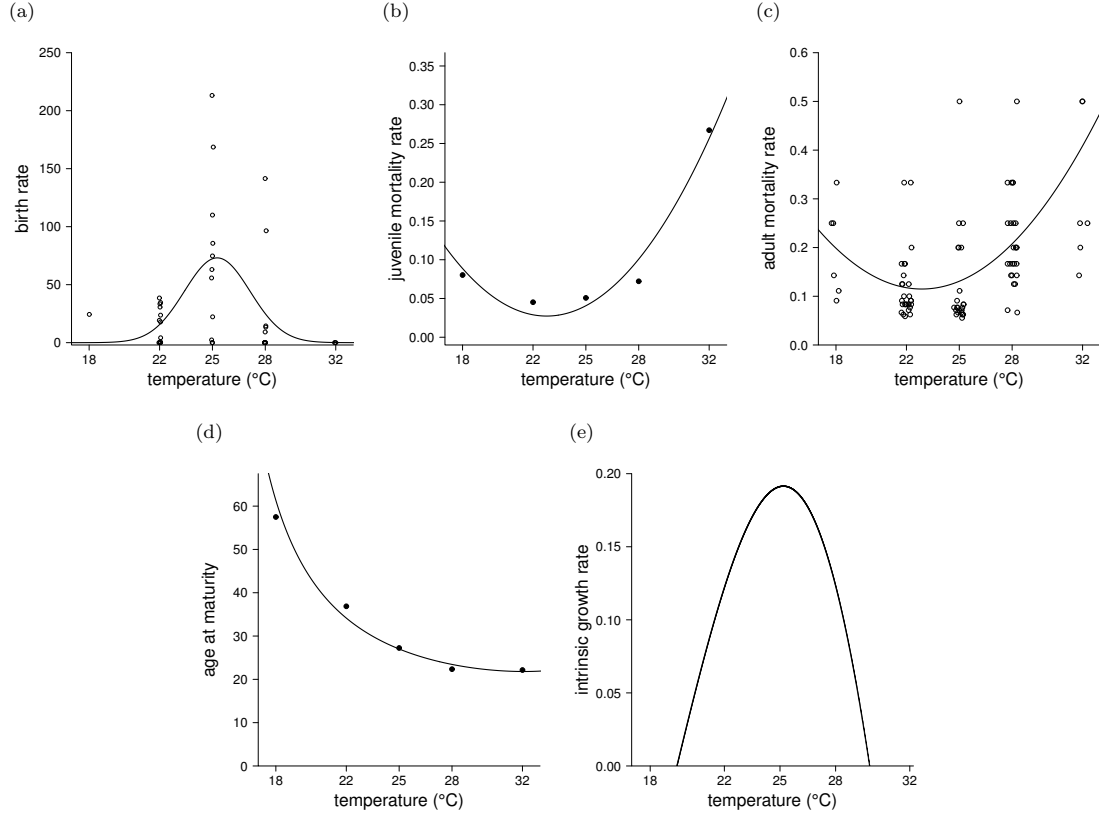


Fig. 2. Temperature responses of life-history traits of *C. includens* in a constant thermal environment. In (a), (b) and (c) the temperature responses of birth rate, and immature and adult mortality rates, respectively. In (d) and (e) the temperature responses of age at maturity and the intrinsic growth rate calculated using the Euler-Lotka equation (3). The graphs are plotted in Celsius degree for easy interpretation but the fittings were done using the temperature in Kelvin. Parameters values are as follows: $b_o = 73.1 \pm 14.18$, $\sigma = 1.86 \pm 0.38$, and $T_o = 298.42 \pm 0.54$ (equation 4); $a_{\bar{d}} = 2.39 \times 10^{-3} \pm 6.08 \times 10^{-4}$, $b_{\bar{d}} = -1.41 \pm 0.36$, and $c_{\bar{d}} = 208.9 \pm 54$ (equation 5 for immature); $a_d = 3.53 \times 10^{-3} \pm 8.02 \times 10^{-4}$, $b_d = -2.09 \pm 0.48$, and $c_d = 309.2 \pm 71.37$ (equation 5 for adult); $a = 2.8 \times 10^{-6} \pm 6.36 \times 10^{-7}$, $\bar{T}_{\min} = 287 \pm 1.12$, $\bar{T}_{\max} = 313.85 \pm 3.56$ (equation 6).

4 CONCLUSIONS AND FURTHER WORK

Two manuscripts already sent to scientific journals are presented in this thesis, opening the way to future work and investigation. The first manuscript enabled me to acquire a robust theoretical learning in mathematical analysis as well as a considerable expertise in computational tools of DDE systems; in turn, the second manuscript permitted me to have a significant background in entomological laboratory, life table data and the use of regression models.

In summary, the first manuscript presents an analytical and numerical analysis about invasion of an *Wolbachia*-infected mosquito population in an area already populated with uninfected mosquitoes. The importance of this study is related to the fact that the infection mediates antiviral protection against a broad range of viruses. The proposed model takes into account several aspects of mosquito life cycle (immature and adult survival, development and oviposition rates) as well as specific features of *Wolbachia* infection on mosquito population (maternal inheritance of bacteria, cytoplasmatic incompatibility, distortion of progeny sex ratio). Differently from other mathematical models already published, our proposition can be easily adapted to consider the influence of abiotic factors on mosquito dynamics. This is important because *Wolbachia* infections in *Ae. aegypti* are vulnerable to high temperatures; heat stress reduces bacteria density in adults and decreases the probability of cytoplasmic incompatibility and maternal transmission. As it is a new model, it is important to discuss the positiveness and boundedness of solutions, as well as the regions of existence and stability of the equilibrium states. We showed that when the delay crosses some thresholds the populations go to extinction. Moreover, its increase can promote, through Hopf bifurcation, stability switch towards instability

for the nonzero equilibria. The overview drawn here, can be used as a safe beginning to input more complex mechanisms on mosquito-bacteria-temperature interaction.

The second manuscript explores the use of statistical and mathematical models to address the relation among temperature and mosquito entomological parameters. The novelty relies on the construction of this relationship for the insect-pest *Chrysodeixis includens*. From this work, we can affirm that the overall cycle of this species is feasible between 19.4 to 29.8 degrees Celsius. Therefore, this species viability is restricted to regions where the annual temperature average is in this range. Furthermore, the optimum temperature value for intrinsic growth rate (25.2 degrees Celsius) is consistent with population outbreaks observed in Brazilian soybean. The results obtained here can be used to forecast accurately the occurrence of different stages of *Chrysodeixis includens* in field and help optimize the control of this insect.

Finally, the knowledge and skills developed throughout my doctorate study are undoubtedly meaningful to carry out interdisciplinary collaboration, in particular with researches from entomology that deal with real data and phenological and/or mathematical models. As an example, the knowledge acquired during the development of the two works described before has been used in the construction of a DDE system to model different stages of *Chrysodeixis includens* life cycle where all parameters depend on temperature. Birth, mortality and developmental models, with fitted parameters coming from the second manuscript, are coupled to this DDE model, whose theoretical background was learned through the first manuscript, in order to get realistic seasonal fluctuations of the populations. Afterwards, control functions simulating insecticide application will be added to the model dynamics. This work is currently underway.

REFERÊNCIAS BIBLIOGRÁFICAS

AHSEN, M. E.; ÖZBAY, H.; NICULESCU, S.-I. Analysis of Gene Regulatory Networks under Positive Feedback. In: VYHLÍDAL, T.; LAFAY, J.-F.; SIPAHI, R. (Ed.). **Delay Systems: From Theory to Numerics and Applications**. Springer International Publishing, 2014. p.127–140.

AVILA, J. L.; BONNET, C.; CLAIRAMBAULT, J.; ÖZBAY, H.; NICULESCU, S.-I.; MERHI, F.; BALLESTA, A.; TANG, R.; MARIE, J.-P. Analysis of a New Model of Cell Population Dynamics in Acute Myeloid Leukemia. In: VYHLÍDAL, T.; LAFAY, J.-F.; SIPAHI, R. (Ed.). **Delay Systems: From Theory to Numerics and Applications**. Springer International Publishing, 2014. p.315–328.

DAMOS, P.; SAVOPOULOU-SOULTANI, M. Temperature-driven models for insect development and vital thermal requirements. **Psyche**, p.1–13, 2012.

JAWORSKI, T.; HILSZCZAŃSKI, J. The effect of temperature and humidity changes on insects development their impact on forest ecosystems in the expected climate change. **Forest Research Papers**, v.74, 2013.

KIM, P. S.; LEVY, D.; LEE, P. P. Modeling and simulations of the immune system as a self regulating network. In: BRAND, M. J. L. (Ed.). **Methods in Enzymology**. Elsevier, 2009. p.79–109.

KRUSZEWSKI, A.; ZHANG, B.; RICHARD, J.-P. Control Design for Teleoperation over Unreliable Networks: A Predictor-Based Approach. In: VYHLÍDAL, T.; LAFAY, J.-F.; SIPAHI, R. (Ed.). **Delay Systems: From Theory to Numerics and Applications**. Springer International Publishing, 2014. p.87–100.

MOORE, B.; ALLARD, G. Climate change impacts on forest health. **Forest Health & Biosecurity Working Papers FBS/34E**, p.49, 2008.

NETHERER, S.; SCHOPF, A. Potential effects of climate change on insect herbivores general aspects and a specific example (Pine processionary moth, *Thaumetopoea pityocampa*). *Forest Ecol Manag.* **Forest Ecology and Management**, v.259, p.831–838, 2010.

OROSZ, G. Decomposing the Dynamics of Delayed Hodgkin-Huxley Neurons. **Delay Systems**, v.1, 2014.

OTTESEN, J. Modelling of the baroreflex-feedback mechanism with time-delay. **Journal of mathematical biology**, v.36, p.41–63, 1997.

PALUMBO, P.; PEPE, P.; PANUNZI, S.; DE GAETANO, A. DDE Model-Based Control of Glycemia via Sub-cutaneous Insulin Administration. In: VYHLÍDAL, T.; LAFAY, J.-F.; SIPAHI, R. (Ed.). **Delay Systems: From Theory to Numerics and Applications**. Springer International Publishing, 2014. p.229–240.